Available online at www.sciencedirect.com
SCIENCE DIRECT
Journal of Sound and Vibration 295 (2006) 964–987
JOURNAL OF SOUND AND VIBRATION
www.elsevier.com/locate/jsvi

Vibration analysis of ring-stiffened cross-ply laminated cylindrical shells

Rong-Tyai Wang*, Zung-Xian Lin

Department of Engineering Science, National Cheng Kung University, Tainan, 701, Taiwan, ROC

Received 28 September 2004; received in revised form 20 March 2005; accepted 31 January 2006
Available online 17 April 2006

Abstract

This work presents the formulation of governing equations for a symmetric cross-ply laminated cylindrical shell with a circumferential stiffener. Two kinds of the circumferential stiffeners are considered: outer ring and inner ring. The effects of rotatory inertia and transverse shearing strain of both the cross-ply laminated shell and stiffener are considered. Further, the warping effect of stiffener also is included. An analytic method is presented to obtain the modal frequencies and their corresponding mode shape functions of the ring-stiffened laminated shell. The orthogonality of two distinct sets of mode shape functions is shown. The effects of inner ring and outer ring on modal frequencies of the ring-stiffened laminated shell are compared. Further, the effect of ply arrangement on modal frequencies of the ring-stiffened shell also is studied. The forced vibration of the ring-stiffened laminated shell due to a concentrated transient force is examined. The stress distributions in the plies of the ring-stiffened laminated shell due to the transient force are investigated.
© 2006 Elsevier Ltd. All rights reserved.

1. Introduction

Laminated cylindrical shells have been widely used in applications such as pipelines, oil containers, oil tankers, pressure vessels, rockets, aircrafts, and submarines. Therefore, it is important to understand the behavior of the laminated shells due to loads, in order that the structures may be used safely in applications. A long laminated cylindrical shell cannot be constructed directly. Fortunately, ring stiffeners can be used to connect many shell parts together for a long laminated cylindrical shell. Most laminated cylindrical shells with ring stiffeners in application are subjected to dynamic loadings. To avoid resonance occurring with the loads, the natural frequencies of a ring-stiffened laminated shell should be known prior to the construction of structure. Therefore, the free-vibration study of a laminated cylindrical shell with ring stiffeners is an important topic in the analysis and design of shell structure.

The free vibration of ring-stiffened cylindrical shells has been studied for many years [1–8]. Usually, the cylindrical shells are regarded as a thin shell, and the rings are considered to be an Euler ring. However, neglecting the effects of transverse shearing strain and the rotatory inertia in both the thin shell and the ring will cause the modal frequencies of a ring-stiffened shell to be overestimated. The errors can be

*Corresponding author. Fax: +886 06 2766549.
E-mail address: rtwang@mail.ncku.edu.tw (R.-T. Wang).

0022-460X/$ - see front matter © 2006 Elsevier Ltd. All rights reserved.
doi:10.1016/j.jsv.2006.01.061

corrected by including the effects of transverse shearing strain and the rotatory inertia in both the shell and the ring [9].

This study presents the displacement fields of a symmetric and cross-ply laminated cylindrical shell with a circumferential isotropic ring stiffener. The displacement fields in the middle surface of laminated shell consist of the axial displacement, the radial displacement and the circumferential displacement. Further, there are two respective rotations of the cross-section along the axial direction and circumferential direction. The ring is considered to be the Timoshenko ring. There are three displacement components along three principal axes of the ring. Further, one bending slope and the twist angle of the ring also are accounted for in this study. The initial curvatures of the laminated shell are supposed to be unchanged during the process of deformation. Further, the stress resultants and stress-couple resultants in both the ring and the cross-ply laminated shell are derived. Via Hamilton's principle, the governing equations and boundary conditions of the ring-stiffened laminated shell are formulated. An analytical method is presented to obtain the modal frequencies and their corresponding sets of mode shape functions of the structure. The orthogonality of any two distinct sets of mode shape functions is derived to show the feasibility of modal analysis. The effect of geometric parameters of the ring on the modal frequencies of the ring-stiffened laminated shell is studied. Further, the effects of outer ring and inner ring on the modal frequencies of the ring-stiffened laminated shell are compared. Moreover, the effect of layer arrangements on the modal frequencies will also be investigated. The method of modal analysis is presented to examine the forced vibration of the ring-stiffened laminated shell. A concentrated transient load on the laminated shell structure is taken as an example. The dynamic stress distribution in the plies of the laminated shell will also be studied.

2. Stress resultants

2.1. Cylindrical shell

A cross-ply laminated cylindrical shell stiffened with an outer ring and an inner ring, respectively, are depicted in Figs. 1(a) and (b). The coordinate system and the displacements of the mid-surface of the laminated shell are depicted in Fig. 2. The stacking sequence and one lamina coordinate system of the laminated shell are depicted in Figs. 3(a) and (b), respectively. The laminated shell has mean radius a, thickness h. The length of the ith span is L_i. The displacements of the middle surface of the ith shell span along the principal axes are denoted as $u^{(i)}$, $v^{(i)}$ and $w^{(i)}$, respectively. Further, $\phi_x^{(i)}\phi_\theta^{(i)}$ are the respective rotation angles of the cross-section along the x-axis and the θ-axis. The displacement fields at a distance ξ from the middle surface in the span are

$$u^{(i)*} = u^{(i)} - \xi\phi_\theta^{(i)}, \quad v^{(i)*} = v^{(i)} + \xi\phi_x^{(i)}, \quad w^{(i)*} = w^{(i)}. \tag{1}$$

By performing the similar procedures described by Kraus [10], the strains are obtained as the forms

$$\varepsilon_x^{(i)} = \varepsilon_{x0}^{(i)} + \xi\kappa_x^{(i)}, \quad \varepsilon_\theta^{(i)} = \varepsilon_{\theta0}^{(i)} + \xi\kappa_\theta^{(i)}, \quad \gamma_{x\theta}^{(i)} = \gamma_{x\theta0}^{(i)} + \xi\kappa_{x\theta}^{(i)},$$

$$\gamma_{xn}^{(i)} = \frac{\partial w^{(i)}}{\partial x} - \phi_\theta^{(i)}, \quad \gamma_{n\theta}^{(i)} = \frac{1}{a}\left(\frac{\partial w^{(i)}}{\partial \theta} - v^{(i)}\right) + \phi_x^{(i)}, \tag{2}$$

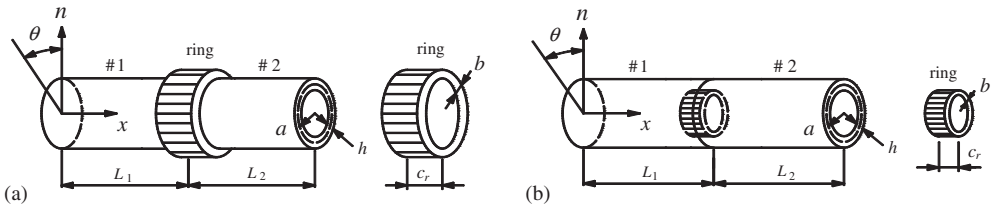

Fig. 1. A laminated cylindrical shell stiffened with a circumferential ring: (a) outer ring and (b) inner ring.

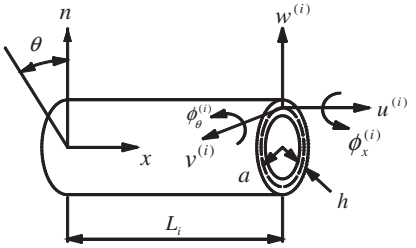

Fig. 2. Geometry and displacements of a laminated cylindrical shell.

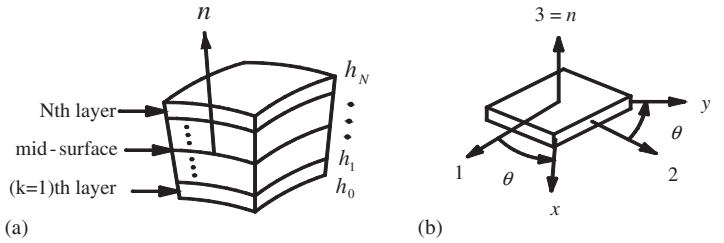

Fig. 3. (a) The stacking sequence and (b) one lamina coordinate system of the laminated shell.

where

$$\varepsilon_{x0}^{(i)}=\frac{\partial u^{(i)}}{\partial x},\quad \varepsilon_{\theta 0}^{(i)}=\frac{1}{a}\left(w^{(i)}+\frac{\partial v^{(i)}}{\partial \theta}\right),\quad \gamma_{x\theta 0}^{(i)}=\frac{\partial v^{(i)}}{\partial x}+\frac{1}{a}\frac{\partial u^{(i)}}{\partial \theta},\quad \kappa_{x}^{(i)}=-\frac{\partial \phi_{\theta}^{(i)}}{\partial x}$$
$$\kappa_{\theta}^{(i)}=\frac{1}{a}\frac{\partial \phi_{x}^{(i)}}{\partial \theta},\quad \kappa_{x\theta}^{(i)}=\frac{\partial \phi_{x}^{(i)}}{\partial x}-\frac{1}{a}\frac{\partial \phi_{\theta}^{(i)}}{\partial \theta}. \tag{3}$$

The stresses in the kth ply of the orthotropic material in the symmetric and cross-ply laminate are [11]

$$\begin{Bmatrix}\tau_x\\ \tau_\theta\\ \tau_{x\theta}\end{Bmatrix}_k^{(i)}=\begin{bmatrix}\bar{Q}_{11} & \bar{Q}_{12} & 0\\ \bar{Q}_{12} & \bar{Q}_{22} & 0\\ 0 & 0 & \bar{Q}_{66}\end{bmatrix}_k^{(i)}\begin{Bmatrix}\varepsilon_x\\ \varepsilon_\theta\\ \gamma_{x\theta}\end{Bmatrix}^{(i)},\quad \begin{Bmatrix}\tau_{n\theta}\\ \tau_{nx}\end{Bmatrix}_k^{(i)}=\begin{bmatrix}\bar{Q}_{44} & 0\\ 0 & \bar{Q}_{55}\end{bmatrix}_k^{(i)}\begin{Bmatrix}\gamma_{n\theta}\\ \gamma_{nx}\end{Bmatrix}^{(i)}, \tag{4}$$

where $\bar{Q}_{lj}$ denotes the stiffness.

The in-plane stress resultants $n_x^{(i)}$, $n_\theta^{(i)}$ and $n_{x\theta}^{(i)}$, the stress-couple resultants $m_x^{(i)}$, $m_\theta^{(i)}$and $m_{x\theta}^{(i)}$, and the transverse stress resultants $q_x^{(i)}$, $q_\theta^{(i)}$ in the laminated shell span are

$$\begin{Bmatrix}n_x^{(i)}\\ n_\theta^{(i)}\end{Bmatrix}=\begin{bmatrix}A_{11}^{(i)} & A_{12}^{(i)}\\ A_{12}^{(i)} & A_{22}^{(i)}\end{bmatrix}\begin{Bmatrix}\varepsilon_{x0}^{(i)}\\ \varepsilon_{\theta 0}^{(i)}\end{Bmatrix},\quad n_{x\theta}^{(i)}=A_{66}^{(i)}\gamma_{x\theta 0}^{(i)}, \tag{5a,b}$$

$$q_x^{(i)}=A_{55}^{(i)}\gamma_{nx}^{(i)},\quad q_\theta^{(i)}=A_{44}^{(i)}\gamma_{n\theta}^{(i)}, \tag{5c,d}$$

$$\begin{Bmatrix}m_x^{(i)}\\ m_\theta^{(i)}\end{Bmatrix}=\begin{bmatrix}D_{11}^{(i)} & D_{12}^{(i)}\\ D_{12}^{(i)} & D_{22}^{(i)}\end{bmatrix}\begin{Bmatrix}\kappa_x^{(i)}\\ \kappa_\theta^{(i)}\end{Bmatrix},\quad m_{x\theta}^{(i)}=D_{66}^{(i)}\kappa_{x\theta}^{(i)}, \tag{5e,f}$$

where

$$A_{11}^{(i)}=\sum_{k=1}^{N}(\bar{Q}_{11})_k^{(i)}(h_k-h_{k-1}),\quad A_{12}^{(i)}=\sum_{k=1}^{N}(\bar{Q}_{12})_k^{(i)}(h_k-h_{k-1}),$$
$$A_{22}^{(i)}=\sum_{k=1}^{N}(\bar{Q}_{12})_k^{(i)}(h_k-h_{k-1}),\quad A_{66}^{(i)}=\sum_{k=1}^{N}(\bar{Q}_{66})_k^{(i)}(h_k-h_{k-1}),$$
$$A_{44}^{(i)}=\sum_{k=1}^{N}(\bar{Q}_{44})_k^{(i)}(h_k-h_{k-1}),\quad A_{55}^{(i)}=\sum_{k=1}^{N}(\bar{Q}_{55})_k^{(i)}(h_k-h_{k-1}),$$
$$D_{11}^{(i)}=\frac{1}{3}\sum_{k=1}^{N}(\bar{Q}_{11})_k^{(i)}(h_k^3-h_{k-1}^3),\quad D_{12}^{(i)}=\frac{1}{3}\sum_{k=1}^{N}(\bar{Q}_{12})_k^{(i)}(h_k^3-h_{k-1}^3),$$
$$D_{22}^{(i)}=\frac{1}{3}\sum_{k=1}^{N}(\bar{Q}_{22})_k^{(i)}(h_k^3-h_{k-1}^3),\quad D_{66}^{(i)}=\frac{1}{3}\sum_{k=1}^{N}(\bar{Q}_{66})_k^{(i)}(h_k^3-h_{k-1}^3) \tag{6}$$

in which h_{k-1} and h_k are the coordinates of the bottom and top surface of the kth ply along the normal direction of laminated shell, respectively.

2.2. Ring

The geometry of displacements of the circumferential ring is depicted in Fig. 4. The ring is assumed to be homogeneous and isotropic, and has density ρ_r, Young's modulus E_r, shear modulus G_r, shear coefficient κ_r, radius R, rectangular cross-sectional area A with width c_r and thickness b, the second moments of area I_x and I_n, torsion coefficient κ_t [12] and torsional rigidity $D_r\left(=k_tG_rc_r^3b\right)$. The displacements on the central line of the ring along the principal axes are denoted as $u^{(3)}$, $v^{(3)}$ and $w^{(3)}$. Further, $\phi_x^{(3)}$ and $\phi_\theta^{(3)}$ are the respective angles of the cross-section along the principal x-axis and θ-axis. The displacements $u^{(3)*}$, $v^{(3)*}$ and $w^{(3)*}$ at any point in the ring along the principal axes are

$$u^{(3)*}=u^{(3)}-\xi\phi_\theta^{(3)},\quad v^{(3)*}=v^{(3)}+\xi\phi_x^{(3)},\quad w^{(3)*}=w^{(3)}+x\phi_\theta^{(3)}. \tag{7}$$

The stress resultants $q_x^{(3)}$, $q_\theta^{(3)}$ and $q_n^{(3)}$, and stress-couple resultants $m_x^{(3)}$, $m_\theta^{(3)}$ and $m_n^{(3)}$of the ring about the principal axes are [13]

$$q_\theta^{(3)}=\frac{E_rA}{R}\left(\frac{\partial v^{(3)}}{\partial\theta}+w^{(3)}\right),\quad q_x^{(3)}=\frac{\kappa_rG_rA}{R}\frac{\partial u^{(3)}}{\partial\theta},\quad q_n^{(3)}=\kappa_rG_rA\left(\phi_x^{(3)}-\frac{v^{(3)}}{R}+\frac{1}{R}\frac{\partial w^{(3)}}{\partial\theta}\right),$$
$$m_x^{(3)}=\frac{E_rI_x}{R}\frac{\partial\phi_x^{(3)}}{\partial\theta},\quad m_n^{(3)}=-\frac{E_rI_n}{R}\phi_\theta^{(3)},\quad m_\theta^{(3)}=\frac{D_r}{R}\frac{\partial\phi_\theta^{(3)}}{\partial\theta}, \tag{8}$$

where $R=a+0.5(b+h)$ for the outer ring, $R=a-0.5(b+h)$ for the inner ring.

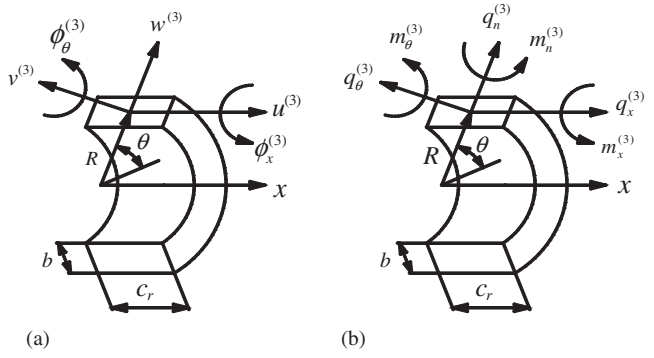

Fig. 4. (a) Displacements and (b) stress resultants of one segment of the circumferential ring.

3. Equations of motion

The strain energy $\bar{S}$ and kinetic energy T of the ring-stiffened cross-ply laminated shell are

$$\bar{S} = \sum_{i=1}^{2} \frac{1}{2} \int_0^{L_i} \int_0^{2\pi} \left[\frac{A_{22}^{(i)} n_x^{(i)2} + A_{11}^{(i)} n_\theta^{(i)2} - 2A_{12}^{(i)} n_x^{(i)} n_\theta^{(i)}}{A_{11}^{(i)} A_{22}^{(i)} - A_{12}^{(i)2}} + \frac{n_{x\theta}^{(i)2}}{A_{66}^{(i)}} + \frac{q_x^{(i)2}}{\kappa A_{55}^{(i)}} + \frac{q_\theta^{(i)2}}{\kappa A_{44}^{(i)}} + \frac{D_{22}^{(i)} m_x^{(i)2} + D_{11}^{(i)} m_\theta^{(i)2} - 2D_{12}^{(i)} m_x^{(i)} m_\theta^{(i)}}{D_{11}^{(i)} D_{22}^{(i)} - D_{12}^{(i)2}} + \frac{m_{x\theta}^{(i)2}}{D_{66}^{(i)}} + \right] a \, \mathrm{d}\theta \, \mathrm{d}x + \frac{1}{2} \int_0^{2\pi} \left\{ \frac{q_\theta^{(3)2}}{E_r A} + \frac{q_n^{(3)2} + q_x^{(3)2}}{\kappa_r G_r A} + \frac{m_x^{(3)2}}{E_r I_x} + \frac{m_n^{(3)2}}{E_r I_n} + \frac{m_\theta^{(3)2}}{D_r} \right\} \Bigg|_{x=L} R \, \mathrm{d}\theta, \tag{9a}$$

$$T = \sum_{i=1}^{2} \frac{\rho}{2} \int_0^{L} \int_0^{2\pi} \left\{ h \left[\left(\frac{\partial u^{(i)}}{\partial t} \right)^2 + \left(\frac{\partial v^{(i)}}{\partial t} \right)^2 + \left(\frac{\partial w^{(i)}}{\partial t} \right)^2 \right] + I \left[\left(\frac{\partial \phi_x^{(i)}}{\partial t} \right)^2 + \left(\frac{\partial \phi_n^{(i)}}{\partial t} \right)^2 \right] \right\} a \, \mathrm{d}\theta \, \mathrm{d}x + \frac{\rho_r}{2} \int_0^{2\pi} \left\{ A \left[\left(\frac{\partial u^{(3)}}{\partial t} \right)^2 + \left(\frac{\partial v^{(3)}}{\partial t} \right)^2 + \left(\frac{\partial w^{(3)}}{\partial t} \right)^2 \right] + I_x \left(\frac{\partial \phi_x^{(3)}}{\partial t} \right)^2 + J \left(\frac{\partial \phi_n^{(3)}}{\partial t} \right)^2 \right\} R \, \mathrm{d}\theta, \tag{9b}$$

where $I(=h^3/12)$ is the area moment of the cross-section of the laminated shell about the mid-surface. The work P done on the laminated shell by the external forces f_x, f_θ and f_n is

$$P = \sum_{i=1}^{2} \int_0^{L} \int_0^{2\pi} \left[f_x \left(u^{(i)} - 0.5h\phi_\theta^{(i)} \right) + f_\theta \left(v^{(i)} + 0.5h\phi_x^{(i)} \right) + f_n w^{(i)} \right] a \, \mathrm{d}\theta \, \mathrm{d}x. \tag{9c}$$

Performing Hamilton's principle yields the following five equations of motion of the cross-ply laminated shell

$$a f_x + a \frac{\partial n_x^{(i)}}{\partial x} + \frac{\partial n_{x\theta}^{(i)}}{\partial \theta} = \rho a h \frac{\partial^2 u^{(i)}}{\partial t^2}, \tag{10a}$$

$$a f_\theta + a \frac{\partial n_{x\theta}^{(i)}}{\partial x} + \frac{\partial n_\theta^{(i)}}{\partial \theta} + q_\theta^{(i)} = \rho a h \frac{\partial^2 v^{(i)}}{\partial t^2}, \tag{10b}$$

$$a f_n + a \frac{\partial q_x^{(i)}}{\partial x} + \frac{\partial q_\theta^{(i)}}{\partial \theta} - n_\theta^{(i)} = \rho a h \frac{\partial^2 w^{(i)}}{\partial t^2}, \tag{10c}$$

$$-\frac{ah}{2} f_x - a \frac{\partial m_x^{(i)}}{\partial x} - \frac{\partial m_{x\theta}^{(i)}}{\partial \theta} + a q_x^{(i)} = \rho a I \frac{\partial^2 \phi_\theta^{(i)}}{\partial t^2}, \tag{10d}$$

$$\frac{ah}{2} f_\theta + a \frac{\partial m_{x\theta}^{(i)}}{\partial x} + \frac{\partial m_\theta^{(i)}}{\partial \theta} - a q_\theta^{(i)} = \rho a I \frac{\partial^2 \phi_x^{(i)}}{\partial t^2}, \quad i = 1, 2, \tag{10e}$$

and the boundary conditions

$$\int_0^{L} \left(n_{x\theta}^{(1)} \delta u^{(1)} + n_\theta^{(1)} \delta v^{(1)} + q_\theta^{(1)} \delta w^{(1)} - m_{x\theta}^{(1)} \delta \phi_\theta^{(1)} + m_\theta^{(1)} \delta \phi_x^{(1)} \right) \Bigg|_0^{2\pi} \mathrm{d}x = 0, \tag{11a}$$

$$\int_0^{L} \left(n_{x\theta}^{(2)} \delta u^{(2)} + n_\theta^{(2)} \delta v^{(2)} + q_\theta^{(2)} \delta w^{(2)} - m_{x\theta}^{(2)} \delta \phi_\theta^{(2)} + m_\theta^{(2)} \delta \phi_x^{(2)} \right) \Bigg|_0^{2\pi} \mathrm{d}x = 0, \tag{11b}$$

$$\int_0^{2\pi} \left[-a \left(n_x^{(1)} \delta u^{(1)} + n_{x\theta}^{(1)} \delta v^{(1)} + q_x^{(1)} \delta w^{(1)} - m_x^{(1)} \delta \phi_\theta^{(1)} + m_{x\theta}^{(1)} \delta \phi_x^{(1)} \right) \right] \Bigg|_{x=0} \mathrm{d}\theta = 0, \tag{11c}$$

$$\int_0^{2\pi}\left[a\left(n_x^{(2)}\delta u^{(2)}+n_{x\theta}^{(2)}\delta v^{(2)}+q_x^{(2)}\delta w^{(2)}-m_x^{(2)}\delta\phi_\theta^{(2)}+m_{x\theta}^{(2)}\delta\phi_x^{(2)}\right)\right]\Big|_{x=L_2}\mathrm{d}\theta=0, \tag{11d}$$

$$\begin{aligned}&\int_0^{2\pi}a\left(n_x^{(1)}\delta u^{(1)}+n_{x\theta}^{(1)}\delta v^{(1)}+q_x^{(1)}\delta w^{(1)}-m_x^{(1)}\delta\phi_\theta^{(1)}+m_{x\theta}^{(1)}\delta\phi_x^{(1)}\right)\Big|_{x=L_1}\mathrm{d}\theta\\&-\int_0^{2\pi}a\left(n_x^{(2)}\delta u^{(2)}+n_{x\theta}^{(2)}\delta v^{(2)}+q_x^{(2)}\delta w^{(2)}-m_x^{(2)}\delta\phi_\theta^{(2)}+m_{x\theta}^{(2)}\delta\phi_x^{(2)}\right)\Big|_{x=0}\mathrm{d}\theta\\&+\int_0^{2\pi}\left\{\left(-\frac{\partial q_x^{(3)}}{\partial\theta}+\rho_rAR\frac{\partial^2u^{(3)}}{\partial t^2}\right)\delta u^{(3)}+\left(-q_n^{(3)}-\frac{\partial q_\theta^{(3)}}{\partial\theta}+\rho_rAR\frac{\partial^2v^{(3)}}{\partial t^2}\right)\delta v^{(3)}\right.\\&+\left(q_\theta^{(3)}-\frac{\partial q_n^{(3)}}{\partial\theta}+\rho_rAR\frac{\partial^2w^{(3)}}{\partial t^2}\right)\delta w^{(3)}+\left(Rq_n^{(3)}-\frac{\partial m_x^{(3)}}{\partial\theta}+\rho_rI_xR\frac{\partial^2\phi_x^{(3)}}{\partial t^2}\right)\delta\phi_x^{(3)}\\&\left.+\left(-m_n^{(3)}-\frac{\partial m_\theta^{(3)}}{\partial\theta}+\rho_rJR\frac{\partial^2\phi_\theta^{(3)}}{\partial t^2}\right)\delta\phi_\theta^{(3)}\right\}\mathrm{d}\theta=0.\end{aligned} \tag{11e}$$

The displacements continuity at the connection of the two-span laminated shell and the ring are

$$\begin{aligned}&\phi_x^{(1)}\big|_{x=L_1}=\phi_x^{(2)}\big|_{x=0}=\phi_x^{(3)},\quad \phi_\theta^{(1)}\Big|_{x=L_1}=\phi_\theta^{(2)}\Big|_{x=0}=\phi_\theta^{(3)},\quad u^{(1)}\big|_{x=L_1}=u^{(2)}\big|_{x=0},\\&v^{(1)}\big|_{x=L_1}=v^{(2)}\big|_{x=0},\quad w^{(1)}\big|_{x=L_1}=w^{(2)}\big|_{x=0}=w^{(3)},\end{aligned} \tag{12a}$$

$$u^{(3)}=\left(u^{(1)}-r_0\phi_\theta^{(1)}\right)\Big|_{x=L_1},\quad v^{(3)}=\left(v^{(1)}+r_0\phi_x^{(1)}\right)\big|_{x=L_1}, \tag{12b}$$

where $r_0=0.5(b+h)$ for the outer ring and $r_0=-0.5(b+h)$ for the inner ring. Employing Eqs. (12a) and (12b) into Eq. (11e) yields the following system of equations of force balances at the conjunction of the ring and the two laminated shells as

$$a\left(n_x^{(1)}\big|_{x=L_1}-n_x^{(2)}\big|_{x=0}\right)-\frac{\partial q_x^{(3)}}{\partial\theta}+\rho_rAR\frac{\partial^2u^{(3)}}{\partial t^2}=0, \tag{13a}$$

$$a\left(n_{x\theta}^{(1)}\Big|_{x=L_1}-n_{x\theta}^{(2)}\Big|_{x=0}\right)-\frac{\partial q_\theta^{(3)}}{\partial\theta}-q_n^{(3)}+\rho_rAR\frac{\partial^2v^{(3)}}{\partial t^2}=0, \tag{13b}$$

$$a\left(q_x^{(1)}\big|_{x=L_1}-q_x^{(2)}\big|_{x=0}\right)+q_\theta^{(3)}-\frac{\partial q_n^{(3)}}{\partial\theta}+\rho_rAR\frac{\partial^2w^{(3)}}{\partial t^2}=0, \tag{13c}$$

$$-a\left(m_x^{(1)}\big|_{x=L_1}-m_x^{(2)}\big|_{x=0}\right)-r_0\left(-\frac{\partial q_x^{(3)}}{\partial\theta}+\rho_rAR\frac{\partial^2u^{(3)}}{\partial t^2}\right)-m_n^{(3)}-\frac{\partial m_\theta^{(3)}}{\partial\theta}+\rho_rJR\frac{\partial^2\phi_\theta^{(3)}}{\partial t^2}=0, \tag{13d}$$

$$\left(m_{x\theta}^{(1)}\Big|_{x=L_1}-m_{x\theta}^{(2)}\Big|_{x=0}\right)+r_0\left(-q_n^{(3)}-\frac{\partial q_\theta^{(3)}}{\partial\theta}+\rho_rAR\frac{\partial^2v^{(3)}}{\partial t^2}\right)+Rq_n^{(3)}-\frac{\partial m_x^{(3)}}{\partial\theta}+\rho_rI_xR\frac{\partial^2\phi_x^{(3)}}{\partial t^2}=0, \tag{13e}$$

where

$$q_\theta^{(3)}=\frac{E_rA}{R}\left\{\frac{\partial}{\partial\theta}\left(v^{(1)}+r_0\phi_x^{(1)}\right)+w^{(1)}\right\}\Big|_{x=L_1},\quad q_x^{(3)}=\frac{\kappa_rG_rA}{R}\frac{\partial}{\partial\theta}\left(u^{(1)}-r_0\phi_\theta^{(1)}\right)\Big|_{x=L_1},$$

$$q_n^{(3)}=\kappa_rG_rA\left\{\phi_x^{(1)}-\frac{1}{R}\left(v^{(1)}+r_0\phi_x^{(1)}\right)+\frac{1}{R}\frac{\partial w^{(1)}}{\partial\theta}\right\}\Big|_{x=L_1},$$

$$m_x^{(3)} = \frac{E_r I_x}{R}\frac{\partial \phi_x^{(1)}}{\partial \theta}\bigg|_{x=L_1}, \quad m_\theta^{(3)} = \frac{D_r}{R}\frac{\partial \phi_\theta^{(1)}}{\partial \theta}\bigg|_{x=L_1}, \quad m_n^{(3)} = -\frac{E_r I_n}{R}\phi_\theta^{(1)}\big|_{x=L_1}. \tag{14}$$

The cross-ply laminated shell is simply connected. Therefore, Eqs. (11a) and (11b) are automatically satisfied. Eqs. (10a)–(10e) constitute the equations of motion of the cross-ply laminated shell with Eqs. (11c) and (11d) being the boundary conditions at two ends. Eqs. (13a)–(13e) describe the forces balance at the connection of the two spans and the ring. Further, Eqs. (12a) and (12b) describe the displacement continuity at the connection of the two spans and the ring.

4. Modal frequencies

To calculate the modal frequencies of the ring-stiffened cross-ply laminated shell, the responses of the ith span shell and those of the ring support are denoted as

$$\begin{aligned}
&\left[u^{(i)}\, w^{(i)}\, \phi_\theta^{(i)}\, n_x^{(i)}\, n_\theta^{(i)}\, q_x^{(i)}\, m_\theta^{(i)}\, m_x^{(i)}\right](x,\theta,t)\\
&\quad = \sin(\omega t)\Big\{\cos(j\theta)\left[U_j^{(i)}\, W_j^{(i)}\, \Phi_{\theta j}^{(i)}\, N_{xj}^{(i)}\, N_{\theta j}^{(i)}\, Q_{xj}^{(i)}\, M_{\theta j}^{(i)}\, M_{xj}^{(i)}\right](x)\\
&\qquad + \sin(j\theta)\left[\bar U_j^{(i)}\, \bar W_j^{(i)}\, \bar\Phi_{\theta j}^{(i)}\, \bar N_{xj}^{(i)}\, \bar N_{\theta j}^{(i)}\, \bar Q_{xj}^{(i)}\, \bar M_{\theta j}^{(i)}\, \bar M_{xj}^{(i)}\right](x)\Big\}.\\
&\qquad + \left[v^{(i)}\, \phi_x^{(i)}\, n_{x\theta}^{(i)}\, q_\theta^{(i)}\, m_{x\theta}^{(i)}\right](x,\theta,t) = \sin(\omega t)\Big\{\sin(j\theta)\left[V_j^{(i)}\, \Phi_{xj}^{(i)}\, N_{x\theta j}^{(i)}\, Q_{\theta j}^{(i)}\, M_{x\theta j}^{(i)}\right](x)
\end{aligned} \tag{15a}$$

$$\cos(j\theta)\left[\bar V_j^{(i)}\, \bar\Phi_{xj}^{(i)}\, \bar N_{x\theta j}^{(i)}\, \bar Q_{\theta j}^{(i)}\, \bar M_{x\theta j}^{(i)}\right](x)\Big\}, \tag{15b}$$

$$\begin{aligned}
&\left\{u^{(3)}\, w^{(3)}\, \phi_\theta^{(3)}\, q_\theta^{(3)}\, m_x^{(3)}\, m_n^{(3)}\right\}(\theta,t)\\
&\quad = \sin(\omega t)\Big\{\cos(j\theta)\Big(U_j^{(3)}\, W_j^{(3)}\, \Phi_{\theta j}^{(3)}\, Q_{\theta j}^{(3)}\, M_{xj}^{(3)}\, M_{nj}^{(3)}\Big)\\
&\qquad + \sin(j\theta)\left[\bar U_j^{(3)}\, \bar W_j^{(3)}\, \bar\Phi_{\theta j}^{(3)}\, \bar Q_{\theta j}^{(3)}\, \bar M_{xj}^{(3)}\, \bar M_{nj}^{(3)}\right]\Big\},
\end{aligned} \tag{15c}$$

$$\begin{aligned}
\left[v^{(3)}\, \phi_x^{(3)}\, q_x^{(3)}\, q_n^{(3)}\, m_\theta^{(3)}\right](\theta,t) = {}& \sin(\omega t)\Big\{\sin(j\theta)\left[V_j^{(3)}\, \Phi_{xj}^{(3)}\, Q_{xj}^{(3)}\, Q_{nj}^{(3)}\, M_{\theta j}^{(3)}\right]\\
&+ \cos(j\theta)\left[\bar V_j^{(3)}\, \bar\Phi_{xj}^{(3)}\, \bar Q_{xj}^{(3)}\, \bar Q_{nj}^{(3)}\, \bar M_{\theta j}^{(3)}\right]\Big\},
\end{aligned} \tag{15d}$$

where the superscript (i) indicates the ith span, the superscript (3) indicates the ring, the subscript j is the number of circumferential waves in the mode shape, ω is the circular frequency and

$$\begin{aligned}
&N_{xj}^{(i)}(x) = A_{11}^{(i)}\frac{\mathrm{d}U_j^{(i)}}{\mathrm{d}x} + A_{12}^{(i)}\frac{1}{a}\left(W_j^{(i)} + jV_j^{(i)}\right), \quad N_{\theta j}^{(i)}(x) = A_{12}^{(i)}\frac{\mathrm{d}U_j^{(i)}}{\mathrm{d}x} + A_{22}^{(i)}\frac{1}{a}\left(W_j^{(i)} + jV_j^{(i)}\right),\\
&N_{x\theta j}^{(i)}(x) = A_{66}^{(i)}\left(\frac{\mathrm{d}V_j^{(i)}}{\mathrm{d}x} - \frac{j}{a}U_j^{(i)}\right), \quad Q_{xj}^{(i)}(x) = \kappa A_{55}^{(i)}\left(\frac{\mathrm{d}W_j^{(i)}}{\mathrm{d}x} - \Phi_{\theta j}^{(i)}\right),\\
&Q_{\theta j}^{(i)}(x) = \kappa A_{44}^{(i)}\left[\Phi_{xj}^{(i)} - \frac{1}{a}\left(V_j^{(i)} + jW_j^{(i)}\right)\right], \quad M_{xj}^{(i)}(x) = -D_{11}^{(i)}\frac{\mathrm{d}\Phi_{\theta j}^{(i)}}{\mathrm{d}x} + D_{12}^{(i)}\frac{j}{a}\Phi_{xj}^{(i)},\\
&M_{\theta j}^{(i)}(x) = -D_{12}^{(i)}\frac{\mathrm{d}\Phi_{\theta j}^{(i)}}{\mathrm{d}x} + D_{22}^{(i)}\frac{j}{a}\Phi_{xj}^{(i)}, \quad M_{x\theta j}^{(i)}(x) = D_{66}^{(i)}\left(\frac{\mathrm{d}\Phi_{xj}^{(i)}}{\mathrm{d}x} + \frac{j}{a}\Phi_{\theta j}^{(i)}\right),\\
&Q_{xj}^{(3)} = -\frac{\kappa_r G_r A}{R}jU_j^{(3)}, \quad Q_{\theta j}^{(3)} = \frac{E_r A}{R}\left(jV_j^{(3)} + W_j^{(3)}\right),
\end{aligned} \tag{16}$$

$$Q_{nj}^{(3)} = \kappa_r G_r A\left(\Phi_{xj}^{(3)} - \frac{V_j^{(3)}}{R} - \frac{j}{R}W_j^{(3)}\right), \quad M_{xj}^{(3)} = \frac{E_r I_x}{R} j\Phi_{xj}^{(1)}(L_1),$$

$$M_{\theta j}^{(3)} = -\frac{D_r}{R} j\Phi_{\theta j}^{(1)}(L_1), \quad M_{nj}^{(3)} = -\frac{E_r I_n}{R}\Phi_{\theta j}^{(1)}(L_1), \tag{17}$$

in which

$$U_j^{(1)}(L_1) = U_j^{(2)}(0), \quad V_j^{(1)}(L_1) = V_j^{(2)}(0), \quad W_j^{(1)}(L_1) = W_j^{(2)}(0) = W_j^{(3)},$$

$$\Phi_{xj}^{(1)}(L_1) = \Phi_{xj}^{(2)}(0) = \Phi_{xj}^{(3)}, \quad \Phi_{\theta j}^{(1)}(L_1) = \Phi_{\theta j}^{(2)}(0) = \Phi_{\theta j}^{(3)},$$

$$U_j^{(3)} = \left(U_j^{(1)} - r_0\Phi_{\theta j}^{(1)}\right)(L_1), \quad V_j^{(3)} = \left(V_j^{(1)} + r_0\Phi_{xj}^{(1)}\right)(L_1). \tag{18}$$

Substituting Eqs. (15a) and (15b) into Eqs. (10a)–(10e) yields

$$-a\frac{\mathrm{d}N_{xj}^{(i)}}{\mathrm{d}x} - jN_{x\theta j}^{(i)} = \rho\omega^2 ahU_j^{(i)}, \quad -a\frac{\mathrm{d}N_{x\theta j}^{(i)}}{\mathrm{d}x} + jN_{\theta j}^{(i)} - Q_{\theta j}^{(i)} = \rho\omega^2 ahV_j^{(i)}, \tag{19a,b}$$

$$-a\frac{\mathrm{d}Q_{xj}^{(i)}}{\mathrm{d}x} - jQ_{\theta j}^{(i)} + N_{\theta j}^{(i)} = \rho\omega^2 ahW_j^{(i)}, \tag{19c}$$

$$a\frac{\mathrm{d}M_{xj}^{(i)}}{\mathrm{d}x} + jM_{x\theta j}^{(i)} - aQ_{xj}^{(i)} = \rho\omega^2 aI\Phi_{\theta j}^{(i)}, \tag{19d}$$

$$-a\frac{\mathrm{d}M_{x\theta j}^{(i)}}{\mathrm{d}x} + jM_{\theta j}^{(i)} + aQ_{\theta j}^{(i)} = \rho\omega^2 aI\Phi_{xj}^{(i)}. \tag{19e}$$

Further, Eqs. (13a)–(13e) can be expressed as

$$-N_{xj}^{(2)}(0) = -N_{xj}^{(1)}(L_1) + \frac{1}{a}\left(jQ_{xj}^{(3)} + \rho_r AR\omega^2 U_j^{(3)}\right), \tag{20a}$$

$$-N_{x\theta j}^{(2)}(0) = -N_{x\theta j}^{(1)}(L_1) + \frac{1}{a}\left(-jQ_{\theta j}^{(3)} + Q_{nj}^{(3)} + \rho_r AR\omega^2 V_j^{(3)}\right), \tag{20b}$$

$$-Q_{xj}^{(2)}(0) = -Q_{xj}^{(1)}(L_1) - \frac{1}{a}\left(Q_{\theta j}^{(3)} - jQ_{nj}^{(3)} - \rho_r AR\omega^2 W_j^{(3)}\right), \tag{20c}$$

$$\begin{aligned} M_{xj}^{(2)}(0) = M_{xj}^{(1)}(L_1) &- \frac{r_0}{a}\left(\rho_r AR\omega^2 U_j^{(3)} + jQ_{xj}^{(3)}\right) \\ &+ \frac{1}{a}\left(M_{nj}^{(3)} + \rho_r JR\omega^2\Phi_{\theta j}^{(3)} + jM_{\theta j}^{(3)}\right). \end{aligned} \tag{20d}$$

$$\begin{aligned} -M_{x\theta j}^{(2)}(0) = &-M_{x\theta j}^{(1)}(L_1) + \frac{r_0}{a}\left(\rho_r AR\omega^2 V_j^{(3)} + Q_{nj}^{(3)} - jQ_{\theta j}^{(3)}\right) \\ &- \frac{1}{a}\left(RQ_{nj}^{(3)} - \rho_r I_x R\omega^2\Phi_{xj}^{(3)} + jM_{xj}^{(3)}\right). \end{aligned} \tag{20e}$$

In the section the operators N_1–N_{17} are listed in Appendix A. Substituting the system of Eqs. (15a), (15b) and (16) into Eqs. (19a)–(19e) yields

$$N_1\left(U_j^{(i)}\right) + j\left(A_{12}^{(i)} + A_{66}^{(i)}\right)\frac{\mathrm{d}V_j^{(i)}}{\mathrm{d}x} + A_{12}^{(i)}\frac{\mathrm{d}W_j^{(i)}}{\mathrm{d}x} = 0, \tag{21a}$$

$$-j\left(A_{12}^{(i)}+A_{66}^{(i)}\right)\frac{\mathrm{d}U_j^{(i)}}{\mathrm{d}x}+N_2\left(V_j^{(i)}\right)-\frac{j}{a}\left(\kappa A_{44}^{(i)}+A_{22}^{(i)}\right)W_j^{(i)}+\kappa A_{44}^{(i)}\Phi_{xj}^{(i)}=0, \tag{21b}$$

$$-A_{12}^{(i)}\frac{\mathrm{d}U_j^{(i)}}{\mathrm{d}x}-\frac{j}{a}\left(A_{22}^{(i)}+\kappa A_{44}^{(i)}\right)V_j^{(i)}+N_3\left(W_j^{(i)}\right)-a\kappa A_{55}^{(i)}\frac{\mathrm{d}\Phi_{\theta j}^{(i)}}{\mathrm{d}x}+j\kappa A_{44}^{(i)}\Phi_{xj}^{(i)}=0, \tag{21c}$$

$$-a\kappa A_{55}^{(i)}\frac{\mathrm{d}W_j^{(i)}}{\mathrm{d}x}+N_4\left(\Phi_{\theta j}^{(i)}\right)+j\left(D_{12}^{(i)}+D_{66}^{(i)}\right)\frac{\mathrm{d}\Phi_{xj}^{(i)}}{\mathrm{d}x}=0, \tag{21d}$$

$$-\kappa A_{44}^{(i)}V_j^{(i)}-j\kappa A_{44}^{(i)}W_j^{(i)}-j\left(D_{12}^{(i)}+D_{66}^{(i)}\right)\frac{\mathrm{d}\Phi_{\theta j}^{(i)}}{\mathrm{d}x}+N_5\left(\Phi_{xj}^{(i)}\right)=0. \tag{21e}$$

The solutions $U_j^{(i)}$, $V_j^{(i)}$, $W_j^{(i)}$, $\Phi_{\theta j}^{(i)}$ and $\Phi_{xj}^{(i)}$ of the system of Eqs. (21a)–(21e) can be obtained and arranged as the vector form

$$\left\{U_j^{(i)},V_j^{(i)},W_j^{(i)},\Phi_{\theta j}^{(i)},\Phi_{xj}^{(i)}\right\}(x)=\sum_{l=1}^{10}a_{lj}^{(i)}\{g_{lj},\bar{g}_{lj},\tilde{g}_{lj},h_{lj},\bar{h}_{lj}\}(x), \tag{22}$$

where $a_{lj}^{(i)}$, $l=1-10$, are constants, and the function $g_{lj}(x)$, $\bar{g}_{lj}(x)$, $\tilde{g}_{lj}(x)$, $h_{lj}(x)$ and $\bar{h}_{lj}(x)$ are the solutions of the following equations:

$$(N_{14}N_{17}-N_{15}N_{16})g_{lj}(x)=0,\quad N_{16}(g_{lj})+N_{17}\left(\frac{\mathrm{d}}{\mathrm{d}x}\bar{g}_{lj}\right)=0, \tag{23a,b}$$

$$\tilde{g}_{lj}=-c_4\bar{g}_{lj}-\frac{1}{A_{12}^{(i)}}\int N_1(g_{lj})\,\mathrm{d}x, \tag{23c}$$

$$h_{lj}(x)=c_3g_{lj}+\int\left[-N_6(\bar{g}_{lj})+N_7(\tilde{g}_{lj})\right]\mathrm{d}x, \tag{23d}$$

$$\bar{h}_{lj}(x)=c_1\frac{\mathrm{d}}{\mathrm{d}x}g_{lj}-\frac{1}{\kappa A_{44}^{(i)}}N_2(\bar{g}_{lj})+c_2\tilde{g}_{lj}(x), \tag{23e}$$

in which the coefficients c_1–c_4 also are listed in Appendix A. Substituting Eq. (22) into Eq. (16) yields

$$\left\{N_{xj}^{(i)},N_{\theta j}^{(i)},N_{x\theta j}^{(i)},Q_{xj}^{(i)},Q_{\theta j}^{(i)}\right\}(x)=\sum_{l=1}^{10}a_{lj}^{(i)}\left\{p_{lj},\bar{p}_{lj},\tilde{p}_{lj},q_{lj},\bar{q}_{lj}\right\}(x),$$

$$\left\{M_{xj}^{(i)},M_{\theta j}^{(i)},M_{x\theta j}^{(i)}\right\}(x)=\sum_{l=1}^{10}a_{lj}^{(i)}\{r_{lj},\bar{r}_{lj},\tilde{r}_{lj}\}(x),\quad i=1,2, \tag{24}$$

where

$$p_{lj}(x)=A_{11}^{(i)}\frac{\mathrm{d}g_{lj}}{\mathrm{d}x}+A_{12}^{(i)}\frac{1}{a}\left(\tilde{g}_{lj}+j\bar{g}_{lj}\right),\quad \bar{p}_{lj}(x)=A_{12}^{(i)}\frac{\mathrm{d}g_{lj}}{\mathrm{d}x}+A_{22}^{(i)}\frac{1}{a}\left(\tilde{g}_{lj}+j\bar{g}_{lj}\right),$$

$$\tilde{p}_{lj}(x)=A_{66}^{(i)}\left(\frac{\mathrm{d}\bar{g}_{lj}}{\mathrm{d}x}-\frac{j}{a}g_{lj}\right),\quad q_{lj}(x)=\kappa A_{55}^{(i)}\left(\frac{\mathrm{d}\tilde{g}_{lj}}{\mathrm{d}x}-h_{lj}\right),$$

$$\bar{q}_{lj}(x)=\kappa A_{44}^{(i)}\left[\bar{h}_{lj}-\frac{1}{a}(j\tilde{g}_{lj}+\bar{g}_{lj})\right],\quad r_{lj}(x)=-D_{11}^{(i)}\frac{\mathrm{d}h_{lj}}{\mathrm{d}x}+D_{12}^{(i)}\frac{j}{a}\bar{h}_{lj},$$

$$\bar{r}_{lj}(x)=-D_{12}^{(i)}\frac{\mathrm{d}h_{lj}}{\mathrm{d}x}+D_{22}^{(i)}\frac{j}{a}\bar{h}_{lj},\quad \tilde{r}_{lj}(x)=D_{66}^{(i)}\left(\frac{\mathrm{d}\bar{h}_{lj}}{\mathrm{d}x}+\frac{j}{a}h_{lj}\right). \tag{25}$$

Setting $x = L_1$ in Eq. (22), then substituting the result into two systems of Eqs. (18) and (17), and arranging the results in two vector forms yield

$$\left\{U_j^{(3)}, V_j^{(3)}, W_j^{(3)}, \Phi_{\theta j}^{(3)}, \Phi_{xj}^{(3)}\right\} = \sum_{l=1}^{10} a_{lj}^{(1)}\{c_{lj}, \bar{c}_{lj}, \tilde{g}_{lj}(L_1), h_{lj}(L_1), \bar{h}_{lj}(L_1)\}, \tag{26a}$$

$$\left\{Q_{\theta j}^{(3)}, Q_{xj}^{(3)}, Q_{nj}^{(3)}, M_{xj}^{(3)}, M_{\theta j}^{(3)}, M_{nj}^{(3)}\right\} = \sum_{l=1}^{10} a_{lj}^{(1)}\{\tilde{c}_{lj}, d_{lj}, \bar{d}_{lj}, \tilde{d}_{lj}, e_{lj}, \tilde{e}_{lj}\}, \tag{26b}$$

where

$$c_{lj} = \left(g_{lj} - r_0 h_{lj}\right)(L_1), \quad \bar{c}_{lj} = \left(\bar{g}_{lj} + r_0 \bar{h}_{lj}\right)(L_1),$$

$$\tilde{c}_{lj} = \frac{E_r A}{R}\left[\tilde{g}_{lj}(L_1) + j\bar{c}_{lj}\right], \quad d_{lj} = -\frac{\kappa_r G_r A}{R} j c_{lj},$$

$$\bar{d}_{lj} = \kappa_r G_r A\left\{\bar{h}_{lj}(L_1) - \frac{1}{R}\left[\bar{c}_{lj} + j\tilde{g}_{lj}(L_1)\right]\right\}, \quad \tilde{d}_{lj} = \frac{E_r I_x}{R} j\bar{h}_{lj}(L_1),$$

$$e_{lj} = -\frac{D_r}{R} j h_{lj}(L_1), \quad \tilde{e}_{lj} = -\frac{E_r I_n}{R} h_{lj}(L_1). \tag{27}$$

Similarly, the following five equations are obtained:

$$\left\{\bar{U}_j^{(i)}, -\bar{V}_j^{(i)}, \bar{W}_j^{(i)}, \bar{\Phi}_{\theta j}^{(i)}, -\bar{\Phi}_{xj}^{(i)}\right\}(x) = \sum_{l=1}^{10} b_{lj}^{(i)}\{g_{lj}, \bar{g}_{lj}, \tilde{g}_{lj}, h_{lj}, \bar{h}_{lj}\}(x), \tag{28a}$$

$$\left\{\bar{N}_{xj}^{(i)}, \bar{N}_{\theta j}^{(i)}, -\bar{N}_{x\theta j}^{(i)}, \bar{Q}_{xj}^{(i)}, -\bar{Q}_{\theta j}^{(i)}\right\}(x) = \sum_{l=1}^{10} b_{lj}^{(i)}\left\{p_{lj}, \bar{p}_{lj}, \tilde{p}_{lj}, q_{lj}, \bar{q}_{lj}\right\}(x), \tag{28b}$$

$$\left\{\bar{M}_{xj}^{(i)}, \bar{M}_{\theta j}^{(i)}, -\bar{M}_{x\theta j}^{(i)}\right\}(x) = \sum_{l=1}^{10} b_{lj}^{(i)}\{r_{lj}, \bar{r}_{lj}, \tilde{r}_{lj}\}(x), \tag{28c}$$

$$\left\{\bar{U}_j^{(3)}, -\bar{V}_j^{(3)}, \bar{W}_j^{(3)}, \bar{\Phi}_{\theta j}^{(3)}, -\bar{\Phi}_{xj}^{(3)}\right\} = \sum_{l=1}^{10} b_{lj}^{(1)}\{c_{lj}, \bar{c}_{lj}, \tilde{g}_{lj}, h_{lj}, \bar{h}_{lj}\}(L_1), \tag{28d}$$

$$\left\{\bar{Q}_{\theta j}^{(3)}, -\bar{Q}_{xj}^{(3)}, -\bar{Q}_{nj}^{(3)}, \bar{M}_{xj}^{(3)}, -\bar{M}_{\theta j}^{(3)}, \bar{M}_{nj}^{(3)}\right\} = \sum_{l=1}^{10} b_{lj}^{(1)}\{\tilde{c}_{lj}, d_{lj}, \bar{d}_{lj}, \tilde{d}_{lj}, e_{lj}, \tilde{e}_{lj}\}(L_1). \tag{28e}$$

The sign conventions for displacements and applied forces at two ends of the ith span are expressed as

$$\{D_L\}_j^{(i)} = \left\{U_j^{(i)} V_j^{(i)} W_j^{(i)} \Phi_{\theta j}^{(i)} \Phi_{xj}^{(i)}\right\}^{\mathrm{T}}(0), \tag{29a}$$

$$\{F_L\}_j^{(i)} = \left\{-N_{xj}^{(i)} - N_{x\theta j}^{(i)} - Q_{xj}^{(i)} M_{xj}^{(i)} - M_{x\theta j}^{(i)}\right\}^{\mathrm{T}}(0), \tag{29b}$$

$$\{D_R\}_j^{(i)} = \left\{U_j^{(i)}\ V_j^{(i)}\ W_j^{(i)}\ \Phi_{\theta j}^{(i)}\ \Phi_{xj}^{(i)}\right\}^{\mathrm{T}}(L_1), \tag{29c}$$

$$\{F_R\}_j^{(i)} = \left\{N_{xj}^{(i)}\, N_{x\theta j}^{(i)}\, Q_{xj}^{(i)} - M_{xj}^{(i)}\, M_{x\theta j}^{(i)}\right\}^{\mathrm{T}}(L_1), \tag{29d}$$

$$\{\bar{D}_L\}_j^{(i)} = \left\{\bar{U}_j^{(i)} - \bar{V}_j^{(i)}\ \bar{W}_j^{(i)}\ \bar{\Phi}_{\theta j}^{(i)} - \bar{\Phi}_{xj}^{(i)}\right\}^{\mathrm{T}}(0), \tag{30a}$$

$$\{\bar{F}_L\}_j^{(i)} = \left\{-\bar{N}_{xj}^{(i)}\ \bar{N}_{x\theta j}^{(i)} - \bar{Q}_{xj}^{(i)}\ \bar{M}_{xj}^{(i)}\ \bar{M}_{x\theta j}^{(i)}\right\}^{\mathrm{T}}(0), \tag{30b}$$

$$\{\bar{D}_R\}_j^{(i)} = \left\{\bar{U}_j^{(i)} - \bar{V}_j^{(i)}\ \bar{W}_j^{(i)}\ \bar{\Phi}_{\theta j}^{(i)} - \bar{\Phi}_{xj}^{(i)}\right\}^{\mathrm{T}}(L_1), \tag{30c}$$

$$\{\bar{F}_R\}_j^{(i)} = \left\{\bar{N}_{xj}^{(i)} - \bar{N}_{x\theta j}^{(i)}\ \bar{Q}_{xj}^{(i)} - \bar{M}_{xj}^{(i)} - \bar{M}_{x\theta j}^{(i)}\right\}^{\mathrm{T}}(L_1). \tag{30d}$$

Substituting Eqs. (22) and (25) into Eqs. (29a)–(29d) and arranging the results yield the following two symbolic forms:

$$\begin{Bmatrix} D_L \\ F_L \end{Bmatrix}_j^{(i)} = [B_j]\{a\}^{(i)}, \quad \begin{Bmatrix} D_R \\ F_R \end{Bmatrix}_j^{(i)} = [G_j]\{a\}^{(i)}, \tag{31a,b}$$

where $\{a\}^{(i)} = \left\{a_{1j}^{(i)}.....a_{10j}^{(i)}\right\}^{\mathrm{T}}$. Similarly, the following two equations are obtained

$$\begin{Bmatrix} \bar{D}_L \\ \bar{F}_L \end{Bmatrix}_j^{(i)} = [B_j]\{b\}^{(i)}, \quad \begin{Bmatrix} \bar{D}_R \\ \bar{F}_R \end{Bmatrix}_j^{(i)} = [G_j]\{b\}^{(i)}, \tag{32a,b}$$

where $\{b\}^{(i)} = \left\{b_{1j}^{(i)}.....b_{10j}^{(i)}\right\}^{\mathrm{T}}$. Solving $\{a\}^{(i)}$ into terms of $\{D_L\}_j^{(i)}$ and $\{F_L\}_j^{(i)}$ from Eq. (31a) then substituting the result into Eq. (31b) yields

$$\begin{Bmatrix} D_R \\ F_R \end{Bmatrix}_j^{(i)} = [H_j]\begin{Bmatrix} D_L \\ F_L \end{Bmatrix}_j^{(i)}, \tag{33}$$

where $[H_j] = [G_j][B_j]^{-1}$. Similarly, the following equation is obtained

$$\begin{Bmatrix} \bar{D}_R \\ \bar{F}_R \end{Bmatrix}_j^{(i)} = [H_j]\begin{Bmatrix} \bar{D}_L \\ \bar{F}_L \end{Bmatrix}_j^{(i)}. \tag{34}$$

Substituting Eqs. (18) and (17) into the system of Eqs. (20a)–(20e) and employing the notations $\{F_L\}_j^{(1)}$, $\{F_R\}_j^{(2)}$ and $\{D_R\}_j^{(1)}$ into the result yield the symbolic form

$$\{F_L\}_j^{(2)} = -\{F_R\}_j^{(1)} + [K]_j\{D_R\}_j^{(1)}, \tag{35}$$

in which the arrays of the matrix $[K]_j$ are listed in Appendix B.

The system of Eq. (18) of displacement continuity at the conjunction of the first span shell and the second span shell is

$$\{D_L\}_j^{(2)} = \{D_R\}_j^{(1)}. \tag{36}$$

Combining Eq. (36) of displacement continuity and Eq. (35) of force balances at the right end of the first shell span, the left end of the second shell span and the ring support yields the symbolic form

$$\begin{Bmatrix} D_L \\ F_L \end{Bmatrix}_j^{(2)} = \begin{bmatrix} I_{5\times5} & O \\ K_j & -I_{5\times5} \end{bmatrix}\begin{Bmatrix} D_R \\ F_R \end{Bmatrix}_j^{(1)}. \tag{37}$$

Substituting Eq. (33) into Eq. (37) yield

$$\begin{Bmatrix} D_L \\ F_L \end{Bmatrix}_j^{(2)} = [Z_j]^{(1)}\begin{Bmatrix} D_L \\ F_L \end{Bmatrix}_j^{(1)}, \tag{38}$$

where the transfer matrix $[Z_j]^{(1)}$ is

$$[Z_j]^{(1)} = \begin{bmatrix} I_{5\times5} & O \\ K_j & -I_{5\times5} \end{bmatrix} [H_j]. \tag{39}$$

Similarly, the following equation is obtained

$$\begin{Bmatrix} \bar{D}_L \\ \bar{F}_L \end{Bmatrix}_j^{(2)} = [Z_j]^{(1)} \begin{Bmatrix} \bar{D}_L \\ \bar{F}_L \end{Bmatrix}_j^{(1)}. \tag{40}$$

Therefore, the response relations at both ends of the entire laminated shell structure are

$$\begin{Bmatrix} D_R \\ F_R \end{Bmatrix}_j^{(2)} = [\tilde{Z}_j]^{(1)} \begin{Bmatrix} D_L \\ F_L \end{Bmatrix}_j^{(1)}, \quad \begin{Bmatrix} \bar{D}_R \\ \bar{F}_R \end{Bmatrix}_j^{(2)} = [\tilde{Z}_j]^{(1)} \begin{Bmatrix} \bar{D}_L \\ \bar{F}_L \end{Bmatrix}_j^{(1)}, \tag{41a,b}$$

where

$$[\tilde{Z}_j]^{(1)} = [H_j][Z_j]^{(1)}. \tag{42}$$

Performing similar procedures of calculation described by Wang and Lin [14], we can obtain the ljth modal frequency ω_{ij} and the corresponding modal shape functions $U_{lj}^{(i)}$, $V_{lj}^{(i)}$, $W_{lj}^{(i)}$, $\Psi_{lj}^{(i)}$, $\Phi_{lj}^{(i)}$, $N_{xlj}^{(i)}$, $N_{x\theta lj}^{(i)}$, $N_{\theta lj}^{(i)}$, $Q_{xlj}^{(i)}$, $Q_{\theta lj}^{(i)}$, $\bar{M}_{xlj}^{(i)}$, $M_{\theta lj}^{(i)}$, $M_{x\theta lj}^{(i)}$, $\bar{U}_{lj}^{(i)}$, $\bar{V}_{lj}^{(i)}$, $\bar{W}_{lj}^{(i)}$, $\bar{\Psi}_{lj}^{(i)}$, $\bar{\Phi}_{lj}^{(i)}$, $\bar{N}_{xlj}^{(i)}$, $\bar{N}_{x\theta lj}^{(i)}$, $\bar{N}_{\theta lj}^{(i)}$, $\bar{Q}_{xlj}^{(i)}$, $\bar{Q}_{\theta lj}^{(i)}$, $\bar{M}_{xlj}^{(i)}$, $\bar{M}_{\theta lj}^{(i)}$ and $\bar{M}_{x\theta\, lj}^{(i)}$ for the ith shell span and $U_{lj}^{(3)}$, $V_{lj}^{(3)}$, $W_{lj}^{(3)}$, $\Psi_{lj}^{(3)}$, $\Phi_{lj}^{(3)}$, $Q_{xlj}^{(3)}$, $Q_{\theta lj}^{(3)}$, $Q_{nlj}^{(3)}$, $M_{xlj}^{(3)}$, $M_{\theta lj}^{(3)}$, $M_{nlj}^{(3)}$, $\bar{U}_{lj}^{(3)}$, $\bar{V}_{lj}^{(3)}$, $\bar{W}_{lj}^{(3)}$, $\bar{\Psi}_{lj}^{(3)}$, $\bar{\Phi}_{lj}^{(3)}$, $\bar{Q}_{xlj}^{(3)}$, $\bar{Q}_{\theta lj}^{(3)}$, $\bar{Q}_{nlj}^{(3)}$, $\bar{M}_{xlj}^{(3)}$, $\bar{M}_{\theta lj}^{(3)}$, and $\bar{M}_{nlj}^{(3)}$, for the ring.

5. Orthogonality

By performing a similar procedure to that described by Wang and Lin [9], the following four equations are obtained:

$$\begin{aligned} &\left\{ \sum_{i=1}^{2} a \int_0^{L_i} \rho \left[h\left(U_{lj}^{(i)} U_{kj}^{(i)} + V_{lj}^{(i)} V_{kj}^{(i)} + W_{lj}^{(i)} W_{kj}^{(i)} \right) I\left(\Phi_{\theta lj}^{(i)} \Phi_{\theta kj}^{(i)} + \Phi_{xlj}^{(i)} \Phi_{xkj}^{(i)} \right) \right] \mathrm{d}x \right. \\ &\left. + \rho_r R \left[A\left(U_{lj}^{(3)} U_{kj}^{(3)} + V_{lj}^{(3)} V_{kj}^{(3)} + W_{lj}^{(3)} W_{kj}^{(3)} \right) + J \Phi_{\theta lj}^{(3)} \Phi_{\theta kj}^{(3)} + I_x \Phi_{xlj}^{(3)} \Phi_{xkj}^{(3)} \right] \right\} = 0, \end{aligned} \tag{43a}$$

$$\begin{aligned} &a \sum_{i=1}^{2} \int_0^{L_i} \left\{ \frac{A_{22}^{(i)} N_{xlj}^{(i)} N_{xkj}^{(i)} + A_{11}^{(i)} N_{\theta lj}^{(i)} N_{\theta kj}^{(i)} - A_{12}^{(i)} \left(N_{xlj}^{(i)} N_{\theta kj}^{(i)} + N_{xkj}^{(i)} N_{\theta lj}^{(i)} \right)}{A_{11}^{(i)} A_{22}^{(i)} - A_{12}^{(i)2}} \right. \\ &\quad + \frac{N_{x\theta lj}^{(i)} N_{x\theta kj}^{(i)}}{A_{66}^{(i)}} + \frac{Q_{xlj}^{(i)} Q_{xkj}^{(i)}}{\kappa A_{55}^{(i)}} + \frac{Q_{\theta lj}^{(i)} Q_{\theta kj}^{(i)}}{\kappa A_{44}^{(i)}} + \frac{M_{x\theta lj}^{(i)} M_{x\theta kj}^{(i)}}{D_{66}^{(i)}} \\ &\quad \left. + \frac{D_{22}^{(i)} M_{xlj}^{(i)} M_{xkj}^{(i)} + D_{11}^{(i)} M_{\theta lj}^{(i)} M_{\theta kj}^{(i)} - D_{12}^{(i)} \left(M_{xlj}^{(i)} M_{\theta kj}^{(i)} + M_{xkj}^{(i)} M_{\theta lj}^{(i)} \right)}{D_{11}^{(i)} D_{22}^{(i)} - D_{12}^{(i)2}} \right\} \mathrm{d}x \\ &\quad + R \left\{ \frac{M_{xlj}^{(3)} M_{xkj}^{(3)}}{E_r I_x} + \frac{Q_{xlj}^{(3)} Q_{xkj}^{(3)} + Q_{nlj}^{(3)} Q_{nkj}^{(3)}}{\kappa_r G_r A} + \frac{M_{\theta lj}^{(3)} M_{\theta kj}^{(3)}}{D_r} + \frac{Q_{\theta lj}^{(3)} Q_{\theta kj}^{(3)}}{E_r A} + \frac{M_{nlj}^{(3)} M_{nkj}^{(3)}}{E_r I_n} \right\} = 0, \end{aligned} \tag{43b}$$

$$\sum_{i=1}^{2} a\int_0^{L_i}\rho\left[h\left(\bar{U}_{lj}^{(i)}\bar{U}_{kj}^{(i)}+\bar{V}_{lj}^{(i)}\bar{V}_{kj}^{(i)}+\bar{W}_{lj}^{(i)}\bar{W}_{kj}^{(i)}\right)+I\left(\bar{\Phi}_{\theta lj}^{(i)}\bar{\Phi}_{\theta kj}^{(i)}+\bar{\Phi}_{xlj}^{(i)}\bar{\Phi}_{xkj}^{(i)}\right)\right]\mathrm{d}x$$
$$+\rho_r R\left[A\left(\bar{U}_{kj}^{(3)}\bar{U}_{kj}^{(3)}+\bar{V}_{lj}^{(3)}\bar{V}_{kj}^{(3)}+\bar{W}_{lj}^{(3)}\bar{W}_{kj}^{(3)}\right)+J\bar{\Phi}_{\theta lj}^{(3)}\bar{\Phi}_{\theta kj}^{(3)}+I_x\bar{\Phi}_{xlj}^{(3)}\bar{\Phi}_{xkj}^{(3)}\right]=0, \tag{43c}$$

$$a\sum_{i=1}^{2}\int_0^{L_i}\left\{\frac{A_{22}^{(i)}\bar{N}_{xlj}^{(i)}\bar{N}_{xkj}^{(i)}+A_{11}^{(i)}\bar{N}_{\theta lj}^{(i)}\bar{N}_{\theta kj}^{(i)}-A_{12}^{(i)}\left(\bar{N}_{xlj}^{(i)}\bar{N}_{\theta kj}^{(i)}+\bar{N}_{xkj}^{(i)}\bar{N}_{\theta lj}^{(i)}\right)}{A_{11}^{(i)}A_{22}^{(i)}-A_{12}^{(i)2}}\right.$$
$$+\frac{\bar{N}_{x\theta lj}^{(i)}\bar{N}_{x\theta kj}^{(i)}}{A_{66}^{(i)}}+\frac{\bar{Q}_{xlj}^{(i)}\bar{Q}_{xkj}^{(i)}}{\kappa A_{55}^{(i)}}+\frac{\bar{Q}_{\theta lj}^{(i)}\bar{Q}_{\theta kj}^{(i)}}{\kappa A_{44}^{(i)}}+\frac{\bar{M}_{x\theta lj}^{(i)}\bar{M}_{x\theta kj}^{(i)}}{D_{66}^{(i)}}$$
$$\left.+\frac{D_{22}^{(i)}\bar{M}_{xlj}^{(i)}\bar{M}_{xkj}^{(i)}+D_{11}^{(i)}\bar{M}_{\theta lj}^{(i)}\bar{M}_{\theta kj}^{(i)}-D_{12}^{(i)}\left(\bar{M}_{xlj}^{(i)}\bar{M}_{\theta kj}^{(i)}+\bar{M}_{xkj}^{(i)}\bar{M}_{\theta lj}^{(i)}\right)}{D_{11}^{(i)}D_{22}^{(i)}-D_{12}^{(i)2}}\right\}\mathrm{d}x$$
$$+R\left\{\frac{\bar{M}_{xlj}^{(3)}\bar{M}_{xkj}^{(3)}}{E_rI_x}+\frac{\bar{Q}_{xlj}^{(3)}\bar{Q}_{xkj}^{(3)}+\bar{Q}_{nlj}^{(3)}\bar{Q}_{nkj}^{(3)}}{\kappa_rG_rA}+\frac{\bar{M}_{\theta lj}^{(3)}\bar{M}_{\theta kj}^{(3)}}{D_r}+\frac{\bar{Q}_{\theta lj}^{(3)}\bar{Q}_{\theta kj}^{(3)}}{E_rA}+\frac{\bar{M}_{nlj}^{(3)}\bar{M}_{nkj}^{(3)}}{E_rI_n}\right\}=0, \tag{43d}$$

for $l\neq k$. Eqs. (43a)–(43d) indicate that corresponding sets of mode shape functions of any two distinct modal frequencies are orthogonal. Further, the ljth modal frequency ω_{lj} is obtained as

$$\omega_{lj}^2=S_{lj}/M_{lj}, \tag{44}$$

where the ljth modal mass M_{lj} and modal stiffness S_{lj} are

$$\begin{aligned}M_{lj}&=\sum_{i=1}^{2}a\int_0^{L_i}\rho\left[h\left(U_{lj}^{(i)2}+V_{lj}^{(i)2}+W_{lj}^{(i)2}\right)+I\left(\Phi_{\theta lj}^{(i)2}+\Phi_{xlj}^{(i)2}\right)\right]\mathrm{d}x\\&\quad+\rho_rR\left[A\left(U_{lj}^{(3)2}+V_{lj}^{(3)2}+W_{lj}^{(3)2}\right)+J\Phi_{\theta lj}^{(3)2}+I_x\Phi_{xlj}^{(3)2}\right]\\&=\sum_{i=1}^{2}a\int_0^{L_i}\rho\left[h\left(\bar{U}_{lj}^{(i)2}+\bar{V}_{lj}^{(i)2}+\bar{W}_{lj}^{(i)2}\right)+I\left(\bar{\Phi}_{\theta lj}^{(i)2}+\bar{\Phi}_{xlj}^{(i)2}\right)\right]\mathrm{d}x\\&\quad+\rho_rR\left[A\left(\bar{U}_{lj}^{(3)2}+\bar{V}_{lj}^{(3)2}+\bar{W}_{lj}^{(3)2}\right)+J\bar{\Phi}_{\theta lj}^{(3)2}+I_x\bar{\Phi}_{xlj}^{(3)2}\right],\end{aligned} \tag{45a}$$

$$\begin{aligned}S_{lj}&=a\sum_{i=1}^{2}\int_0^{L_i}\left\{\frac{A_{22}^{(i)}N_{xlj}^{(i)2}+A_{11}^{(i)}N_{\theta lj}^{(i)2}-2A_{12}^{(i)}N_{xlj}^{(i)}N_{\theta lj}^{(i)}}{A_{11}^{(i)}A_{22}^{(i)}-A_{12}^{(i)2}}+\frac{N_{x\theta lj}^{(i)2}}{A_{66}^{(i)}}+\frac{Q_{xlj}^{(i)2}}{\kappa A_{55}^{(i)}}+\frac{Q_{\theta lj}^{(i)2}}{\kappa A_{44}^{(i)}}+\frac{M_{x\theta lj}^{(i)2}}{D_{66}^{(i)}}\right.\\&\quad\left.+\frac{D_{22}^{(i)}M_{xlj}^{(i)2}+D_{11}^{(i)}M_{\theta lj}^{(i)2}-2D_{12}^{(i)}M_{xlj}^{(i)}M_{\theta lj}^{(i)}}{D_{11}^{(i)}D_{22}^{(i)}-D_{12}^{(i)2}}\right\}\mathrm{d}x\\&\quad+R\left\{\frac{M_{xlj}^{(3)2}}{E_rI_x}+\frac{Q_{xlj}^{(3)2}+Q_{nlj}^{(3)2}}{\kappa_rG_rA}+\frac{M_{\theta lj}^{(3)2}}{D_r}+\frac{Q_{\theta lj}^{(3)2}}{E_rA}+\frac{M_{nlj}^{(3)2}}{E_rI_n}\right\}\\&=a\sum_{i=1}^{2}\int_0^{L_i}\left\{\frac{A_{22}^{(i)}\bar{N}_{xlj}^{(i)2}+A_{11}^{(i)}\bar{N}_{\theta lj}^{(i)2}-2A_{12}^{(i)}\bar{N}_{xlj}^{(i)}\bar{N}_{\theta lj}^{(i)}}{A_{11}^{(i)}A_{22}^{(i)}-A_{12}^{(i)2}}+\frac{\bar{N}_{x\theta lj}^{(i)}}{A_{66}^{(i)}}+\frac{\bar{Q}_{xlj}^{(i)2}}{\kappa A_{55}^{(i)}}+\frac{\bar{Q}_{\theta lj}^{(i)2}}{\kappa A_{44}^{(i)}}+\frac{\bar{M}_{x\theta lj}^{(i)}}{D_{66}^{(i)}}\right.\\&\quad\left.+\frac{D_{22}^{(i)}\bar{M}_{xlj}^{(i)2}+D_{11}^{(i)}\bar{M}_{\theta lj}^{(i)2}-2D_{12}^{(i)}\bar{M}_{xlj}^{(i)}\bar{M}_{\theta lj}^{(i)}}{D_{11}^{(i)}D_{22}^{(i)}-D_{12}^{(i)2}}\right\}\mathrm{d}x\\&\quad+R\left\{\frac{\bar{M}_{xlj}^{(3)2}}{E_rI_x}+\frac{\bar{Q}_{xlj}^{(3)2}+\bar{Q}_{nlj}^{(3)2}}{\kappa_rG_rA}+\frac{\bar{M}_{\theta lj}^{(3)2}}{D_r}+\frac{\bar{Q}_{\theta lj}^{(3)2}}{E_rA}+\frac{\bar{M}_{nlj}^{(3)2}}{E_rI_n}\right\}.\end{aligned} \tag{45b}$$

6. Forced vibration

While examining the forced vibration, the responses of the ring-stiffened cross-ply laminated shell can be expressed by the mode superposition in the following forms:

$$\begin{aligned}&\left\{u^{(i)}\ w^{(i)}\ \phi_\theta^{(i)}\ n_x^{(i)}\ n_\theta^{(i)}\ q_x^{(i)}\ m_\theta^{(i)}\ m_x^{(i)}\right\}(x,\theta,t)\\&\quad=\sum_{l=1,j=0}\left\{C_{lj}(t)\cos(j\theta)\left[U_{lj}^{(i)}\ W_{lj}^{(i)}\ \Phi_{\theta lj}^{(i)}\ N_{xlj}^{(i)}\ N_{\theta lj}^{(i)}\ Q_{xlj}^{(i)}\ M_{\theta lj}^{(i)}\ M_{xlj}^{(i)}\right](x)\right.\\&\qquad\left.+\bar{C}_{lj}(t)\sin(j\theta)\left[\bar{U}_{lj}^{(i)}\ \bar{W}_{lj}^{(i)}\ \bar{\Phi}_{\theta lj}^{(i)}\ \bar{N}_{xj}^{(i)}\ \bar{N}_{\theta lj}^{(i)}\ \bar{Q}_{xlj}^{(i)}\ \bar{M}_{\theta lj}^{(i)}\ \bar{M}_{xlj}^{(i)}\right](x)\right\},\end{aligned}\tag{46a}$$

$$\begin{aligned}&\left\{v^{(i)}\ \phi_x^{(i)}\ n_{x\theta}^{(i)}\ q_\theta^{(i)}\ m_{x\theta}^{(i)}\right\}(x,\theta,t)\\&\quad=\sum_{l=1,j=0}\left\{C_{lj}(t)\sin(j\theta)\left[V_{lj}^{(i)}\ \Phi_{xlj}^{(i)}\ N_{x\theta lj}^{(i)}\ Q_{\theta lj}^{(i)}\ M_{x\theta lj}^{(i)}\right](x)\right.\\&\qquad\left.+\bar{C}_{lj}(t)\cos(j\theta)\left[\bar{V}_{lj}^{(i)}\ \bar{\Phi}_{xlj}^{(i)}\ \bar{N}_{x\theta lj}^{(i)}\ \bar{Q}_{\theta lj}^{(i)}\ \bar{M}_{x\theta lj}^{(i)}\right](x)\right\},\end{aligned}\tag{46b}$$

for the ith shell span and

$$\begin{aligned}&\left\{u^{(3)}\ v^{(3)}\ w^{(3)}\ \phi_\theta^{(3)}\ \phi_x^{(3)}\ q_x^{(3)}\ q_\theta^{(3)}\ q_n^{(3)}\ m_\theta^{(3)}\ m_x^{(3)}\ m_n^{(3)}\right\}(\theta,t)\\&\quad=\sum_{l=1,j=0}\left\{C_{lj}(t)\cos(j\theta)\left[U_{lj}^{(3)}\ \bar{V}_{lj}^{(3)}\ W_{lj}^{(3)}\ \Phi_{\theta lj}^{(3)}\ \bar{\Phi}_{xlj}^{(3)}\ \bar{Q}_{xlj}^{(3)}\ Q_{\theta lj}^{(3)}\ \bar{Q}_{nlj}^{(3)}\ \bar{M}_{\theta lj}^{(3)}\ M_{xlj}^{(3)}\ M_{nlj}^{(3)}\right]\right.\\&\qquad\left.+\bar{C}_{lj}(t)\sin(j\theta)\left[\bar{U}_{lj}^{(3)}\ V_{lj}^{(3)}\ \bar{W}_{lj}^{(3)}\ \bar{\Phi}_{\theta lj}^{(3)}\ \Phi_{xlj}^{(3)}\ Q_{xlj}^{(3)}\ \bar{Q}_{\theta lj}^{(3)}\ Q_{nlj}^{(3)}\ M_{\theta lj}^{(3)}\ \bar{M}_{xlj}^{(3)}\ \bar{M}_{nlj}^{(3)}\right]\right\},\end{aligned}\tag{46c}$$

for the ring. $C_{lj}(t)$ and $\bar{C}_{lj}(t)$ are the ljth modal amplitudes of the entire structure. Performing similar procedures to those described by Wang and Lin [14] and employing the orthogonality of any two distinct sets of mode shape functions into the results yields

$$M_{lj}\left(\ddot{C}_{lj},\ddot{\bar{C}}_{lj}\right)+S_{lj}\left(C_{lj},\bar{C}_{lj}\right)=\left(F_{lj},\bar{F}_{lj}\right)(t),\tag{47}$$

in which $(\dot{\ })$ indicates the differentiation with respect to time, the ljth modal excitations $F_{lj}(t)$ and $\bar{F}_{lj}(t)$, and the initial conditions $C_{ij}(0)$, $\dot{C}_{lj}(0)$, $\bar{C}_{lj}(0)$ and $\dot{\bar{C}}_{lj}(0)$ are given, respectively, as

$$\begin{aligned}F_{lj}(t)=\frac{1}{\pi}\sum_{i=1}^{2}\int_0^{L_i}\int_0^{2\pi}a\left\{\cos(j\theta)\left(f_x U_{lj}^{(i)}+f_n W_{lj}^{(i)}-\frac{h}{2}f_x\Phi_{\theta lj}^{(i)}\right)\right.\\\left.+\sin(j\theta)\left(V_{lj}^{(i)}+\frac{h}{2}\Phi_{xlj}^{(i)}\right)f\right\}\mathrm{d}\theta\,\mathrm{d}x,\end{aligned}\tag{48a}$$

$$\begin{aligned}\bar{F}_{lj}(t)=\frac{1}{\pi}\sum_{i=1}^{2}\int_0^{L_i}\int_0^{2\pi}a\left\{\sin(j\theta)\left(f_x \bar{U}_{lj}^{(i)}+f_n \bar{W}_{lj}^{(i)}-\frac{h}{2}f_x\bar{\Phi}_{\theta lj}^{(i)}\right)\right.\\\left.+\cos(j\theta)\left(\bar{V}_{lj}^{(i)}+\frac{h}{2}\bar{\Phi}_{xlj}^{(i)}\right)f_\theta\right\}\mathrm{d}\theta\,\mathrm{d}x,\end{aligned}\tag{48b}$$

$$C_{kj}(0)=\frac{1}{\pi M_{kj}}\int_0^{2\pi}\rho\sum_{i=1}^{2}a\int_0^{L_i}\Big\{h\Big[u^{(i)}U_{kj}^{(i)}\cos(j\theta)+v^{(i)}V_{kj}^{(i)}\sin(j\theta)+w^{(i)}W_{kj}^{(i)}\cos(j\theta)\Big]+I\Big[\phi_\theta^{(i)}\Phi_{\theta kj}^{(i)}\cos(j\theta)+\phi_x^{(i)}\Phi_{xkj}^{(i)}\sin(j\theta)\Big]\Big\}\Big|_{t=0}\,\mathrm{d}x\,\mathrm{d}\theta+\frac{1}{\pi M_{kj}}\int_0^{2\pi}\rho_r R\Big\{A\Big[u^{(3)}U_{kj}^{(3)}\cos(j\theta)+v^{(3)}V_{kj}^{(3)}\sin(j\theta)+w^{(3)}W_{kj}^{(3)}\cos(j\theta)\Big]+J\phi_\theta^{(3)}\Phi_{\theta kj}^{(3)}\cos(j\theta)+I_x\phi_x^{(3)}\Phi_{xkj}^{(3)}\sin(j\theta)\Big\}\Big|_{t=0}\,\mathrm{d}\theta, \tag{49a}$$

$$\dot{C}_{kj}(0)=\frac{1}{\pi M_{kj}}\int_0^{2\pi}\rho\sum_{i=1}^{2}a\int_0^{L_i}\Big\{h\Big[\dot{u}^{(i)}U_{kj}^{(i)}\cos(j\theta)+\dot{v}^{(i)}V_{kj}^{(i)}\sin(j\theta)+\dot{w}^{(i)}W_{kj}^{(i)}\cos(j\theta)\Big]+I\Big[\dot{\phi}_\theta^{(i)}\Phi_{\theta kj}^{(i)}\cos(j\theta)+\dot{\phi}_x^{(i)}\Phi_{xkj}^{(i)}\sin(j\theta)\Big]\Big\}\Big|_{t=0}\,\mathrm{d}x\,\mathrm{d}\theta+\frac{1}{\pi M_{kj}}\int_0^{2\pi}\rho_r R\Big\{A\Big[\dot{u}^{(3)}U_{kj}^{(3)}\cos(j\theta)+\dot{v}^{(3)}V_{kj}^{(3)}\sin(j\theta)+\dot{w}^{(3)}W_{kj}^{(3)}\cos(j\theta)\Big]+J\dot{\phi}_\theta^{(3)}\Phi_{\theta kj}^{(3)}\cos(j\theta)+I_x\dot{\phi}_x^{(3)}\Phi_{xkj}^{(3)}\sin(j\theta)\Big\}\Big|_{t=0}\,\mathrm{d}\theta, \tag{49b}$$

$$\bar{C}_{kj}(0)=\frac{1}{\pi M_{kj}}\int_0^{2\pi}\rho\sum_{i=1}^{2}a\int_0^{L_i}\Big\{h\Big[u^{(i)}\bar{U}_{kj}^{(i)}\sin(j\theta)+v^{(i)}\bar{V}_{kj}^{(i)}\cos(j\theta)+w^{(i)}\bar{W}_{kj}^{(i)}\sin(j\theta)\Big]+I\Big[\phi_\theta^{(i)}\bar{\Phi}_{\theta kj}^{(i)}\sin(j\theta)+\phi_x^{(i)}\bar{\Phi}_{xkj}^{(i)}\cos(j\theta)\Big]\Big\}\Big|_{t=0}\,\mathrm{d}x\,\mathrm{d}\theta+\frac{1}{\pi M_{kj}}\int_0^{2\pi}\rho_r R\Big\{A\Big[u^{(3)}\bar{U}_{kj}^{(3)}\sin(j\theta)+v^{(3)}\bar{V}_{kj}^{(3)}\cos(j\theta)+w^{(3)}\bar{W}_{kj}^{(3)}\sin(j\theta)\Big]+J\phi_\theta^{(3)}\bar{\Phi}_{\theta kj}^{(3)}\sin(j\theta)+I_x\phi_x^{(3)}\bar{\Phi}_{xkj}^{(3)}\cos(j\theta)\Big\}\Big|_{t=0}\,\mathrm{d}\theta, \tag{49c}$$

$$\dot{\bar{C}}_{kj}(0)=\frac{1}{\pi M_{kj}}\int_0^{2\pi}\rho\sum_{i=1}^{2}a\int_0^{L_i}\Big\{h\Big[\dot{u}^{(i)}\bar{U}_{kj}^{(i)}\sin(j\theta)+\dot{v}^{(i)}\bar{V}_{kj}^{(i)}\cos(j\theta)+\dot{w}^{(i)}\bar{W}_{kj}^{(i)}\sin(j\theta)\Big]+I\Big[\dot{\phi}_\theta^{(i)}\bar{\Phi}_{\theta kj}^{(i)}\sin(j\theta)+\dot{\phi}_x^{(i)}\bar{\Phi}_{xkj}^{(i)}\cos(j\theta)\Big]\Big\}\Big|_{t=0}\,\mathrm{d}x\,\mathrm{d}\theta+\frac{1}{\pi M_{kj}}\int_0^{2\pi}\rho_r R\Big\{A\Big[\dot{u}^{(3)}\bar{U}_{kj}^{(3)}\sin(j\theta)+\dot{v}^{(3)}\bar{V}_{kj}^{(3)}\cos(j\theta)+\dot{w}^{(3)}\bar{W}_{kj}^{(3)}\sin(j\theta)\Big]+J\dot{\phi}_\theta^{(3)}\bar{\Phi}_{\theta kj}^{(3)}\sin(j\theta)+I_x\dot{\phi}_x^{(3)}\bar{\Phi}_{xkj}^{(3)}\cos(j\theta)\Big\}\Big|_{t=0}\,\mathrm{d}\theta. \tag{49d}$$

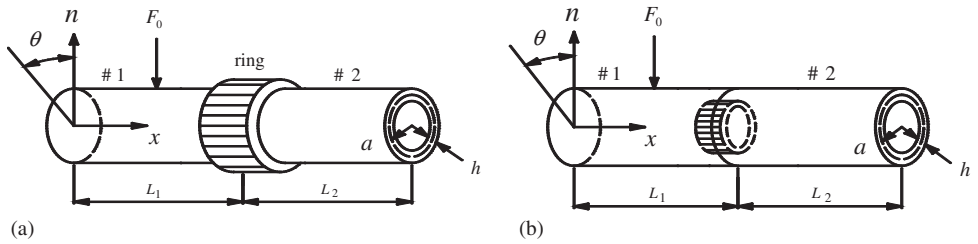

Fig. 5. A concentrated force acts on the laminated cylindrical shell stiffened with a circumferential ring: (a) outer ring and (b) inner ring.

A concentrated transient load magnitude of F_0 acting at the point $(\theta = 0, x = 0.5L_1)$ of the first shell span is displayed in Fig. 5. The form of the load is

$$f_n(t) = \begin{cases} F_0\delta(x - L_1/2, \theta)\sin(\pi t), & 0 \leqslant t \leqslant 1\,\text{s}, \\ 0, & 1\,\text{s} \leqslant t. \end{cases} \tag{50}$$

Substituting Eq. (50) into Eqs. (48a) and (48b) yields the respective histories of $\bar{F}_{lj}(t)$ and $F_{lj}(t)$. The respective histories of $C_{lj}(t)$, $\dot{C}_{lj}(t)$, $\bar{C}_{lj}(t)$ and $\ddot{\bar{C}}_{lj}(t)$ can be obtained by substituting $\bar{F}_{lj}(t)$ and $F_{lj}(t)$ into Eq. (47) then performing similar procedures to those described by Wang [15].

7. Examples and discussion

In this section, the constants $E_{11} = 150\,\text{GPa}$, $E_{22} = E_{33} = 9\,\text{GPa}$, $G_{23} = 2.5\,\text{GPa}$, $G_{12} = G_{13} = 7.1\,\text{GPa}$, $\upsilon_{12} = \upsilon_{31} = \upsilon_{23} = 0.3$, longitudinal tensile strength $X_t = 1.5\,\text{GPa}$, longitudinal compressive strength $X_c = 1.6\,\text{GPa}$, transverse tensile strength $Y_t = 44.5\,\text{MPa}$, transverse compressive strength $Y_c = 253\,\text{MPa}$, shear strength $S = 41.4\,\text{MPa}$ and $\rho = 1.6\,\text{Mg/m}^3$ of T300/976 graphite-epoxy [16] for the cross-ply laminated shells $(L = 5\,\text{m}, h = 3\,\text{cm}, L_1 = L_2 = 205\,\text{m})$ are considered. Further, the constants $E_r = 70\,\text{GPa}$, $G_r = 2.6\,\text{GPa}$, $\rho_r = 2.71\,\text{Mg/m}^3$, $\kappa_t = 0.23$ and $\kappa_r = 0.833$ of 6061-T6 aluminum rings are also considered. The magnitude of the concentrated transient force is $F_0 = 1\,\text{N}$. The laminated shells have both ends being fixed. The loading point $(\theta = 0, x = 1.25\,\text{m})$ is considered in the analysis of forced vibration for the ring-stiffened laminated shell. Further, the stresses distribution in each ply along the line of acting force is considered.

7.1. Without ring

The lowest four circumferential modes of the $[0/90/0]_s$ laminated shell are depicted in Fig. 6. The lowest axial modes of the cross-ply laminated shell are displayed in Fig. 7. The cross-section is uniformly expanded or contracted for $j = 0$, and is in the state of rigid body motion for $j = 1$. Further, the cross-section will be deformed for j being greater than 1. The cross-section of the laminated shell is in the state of rigid-body motion for the modes (1, 1), and (2, 1). In the situation, the laminated shell behaves like a hollow beam. Moreover, the radius of the laminated shell will be the radius of gyration of a hollow beam. Therefore, the larger radius implies larger ω_{11} and ω_{21} of the laminated shell as indicated in Table 1. The cross-section of the laminated shell is deformed for the modes (1, 2) and (2, 2). The larger radius induces the less coupling between W or V and U of the laminated shell. Therefore, results in Table 1 indicates that the larger radius implies less ω_{12} and ω_{22}.

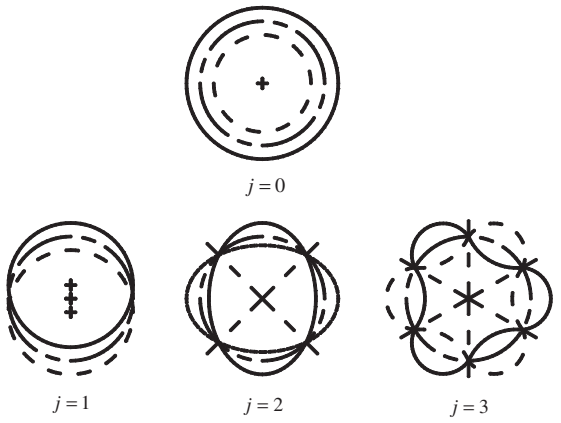

Fig. 6. The lowest four circumferential mode shapes of the $[90/0/90]_s$ laminated cylindrical shell ($a = 30\,\text{cm}$).

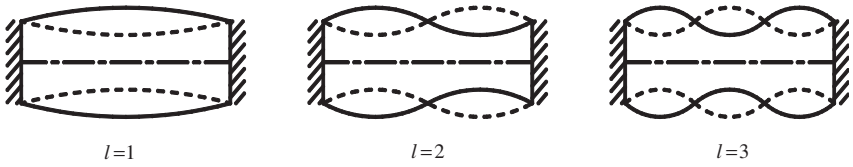

Fig. 7. The lowest three axial mode shapes of the $[90/0/90]_s$ laminated cylindrical shell ($a = 30$ cm).

Table 1
The radius a (cm) effect on the comparison of the modal frequencies (rad/s) of the $[90/0/90]_s$ laminated shell ($L = 5$ m, $h = 3$ cm)

a	ω_{10}	ω_{11}	ω_{21}	ω_{12}	ω_{22}
30	3754.9	725.4	1542.0	2143.2	2257.9
35	3756.1	768.8	1592.4	1610.9	1778.7
40	3756.7	801.1	1633.1	1269.8	1496.8

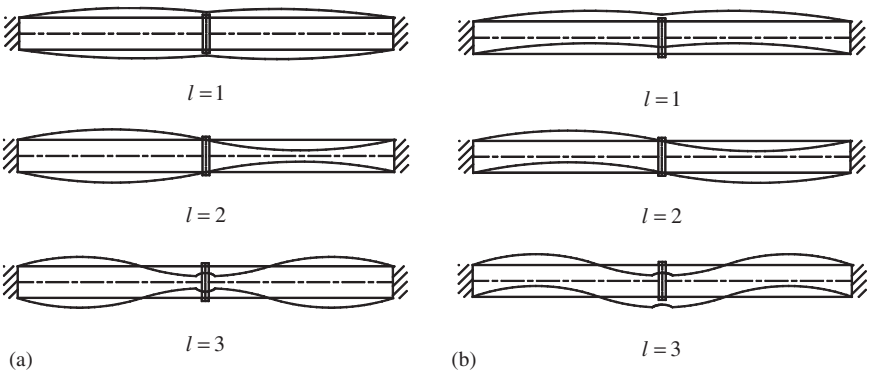

Fig. 8. The lowest three axial mode shapes of the $[90/0/90]_s$ laminated cylindrical shell ($a = 30$ cm) with an outer stiffening ring: (a) j is an even number and (b) j is an odd number.

Table 2
The layers effect on the comparison of the modal frequencies (rad/s) of the laminated shell ($L = 5$ m, $h = 3$ cm, $a = 30$ cm)

Layer	ω_{10}	ω_{11}	ω_{21}	ω_{12}	ω_{22}
$[0/90/0]_s$	4906.7	805.1	1655.0	1427.8	1653.7
$[90/0/90]_s$	3754.8	725.4	1542.0	2143.2	2257.9

The shape of cross-section of the cross-ply laminated shell ($\alpha = 30$ cm) does not change for the modes (1, 0), (1, 1) and (2, 1) (Fig. 8). Further, the laminated shell is in the state of bending modes along the axial direction for these modes. However, the cross-section of the laminated shell is deformed for the modes (1, 2) and (2, 2). The shell with the $[0/90/0]_s$ lamination gives a larger bending rigidity, however, smaller transverse shear stiffness than the shell with the $[90/0/90]_s$ lamination does. Therefore, the $[0/90/0]_s$ laminated shell has larger ω_{10}, ω_{11} and ω_{21}, however, less ω_{12} and ω_{22} than those of the $[90/0/90]_s$ laminated shell as indicated in Table 2.

In the following sections, the mean radius $\alpha = 30$ cm of the cross-ply laminated shells is considered. Results obtained by the method of modal analysis converge rather fast. Therefore, it is sufficient to employ ω_{10}, ω_{11}, ω_{21}, ω_{12}, ω_{22} and their corresponding sets of mode shape functions of the cross-ply laminated shell with a stiffening ring in the method of modal analysis in the numerical computation.

Table 3
The thickness b (cm) effect of outer ring ($c_r = 3$ cm) on the comparison of the modal frequencies (rad/s) of the ring-stiffened $[90/0/90]_s$ laminated shell ($L_1 = L_2 = 2.5$ m, $a = 30$ cm, $h = 3$ cm)

b	ω_{10}	ω_{11}	ω_{21}	ω_{12}	ω_{22}
1	3745.3	723.1	1544.7	2147.3	2263.4
2	3731.6	720.2	1549.2	2161.9	2268.7
3	3717.4	717.2	1553.7	2182.7	2273.7

Table 4
The width c_r (cm) effect of outer ring ($b = 3$ cm) on the comparison of the modal frequencies (rad/s) of the ring-stiffened $[90/0/90]_s$ laminated shell ($L_1 = L_2 = 2.5$ m, $a = 30$ cm, $h = 3$ cm)

c_r	ω_{10}	ω_{11}	ω_{21}	ω_{12}	ω_{22}
3	3717.4	717.2	1553.7	2182.7	2273.7
6	3676.5	708.6	1565.3	2194.2	2283.1
9	3636.3	700.3	1575.2	2196.7	2288.8

Table 5
The layers effect on the comparison of the modal frequencies (rad/s) of the laminated shell ($L_1 = L_2 = 2.5$ m, $a = 30$ cm, $h = 3$ cm) with an outer stiffening ring ($b = 3$ cm, $c_r = 6$ cm)

Layer	ω_{10}	ω_{11}	ω_{21}	ω_{12}	ω_{22}
$[0/90/0]_s$	4695.2	787.1	1667.7	1530.2	1673.0
$[90/0/90]_s$	3676.5	708.6	1565.3	2194.2	2283.1

7.2. Outer ring

The fundamental three axial modes along the axis of the $[90/0/90]_s$ laminated shell with an outer stiffening ring for j being an even number and an odd number are depicted in Figs. 8(a) and (b), respectively. These figures show the ring induces a constraint on the transverse deformation of the shell. Therefore, the effects of width and thickness of a stiffening ring on the modal frequencies of the combined structure are studied. The comparisons of modal frequencies of the $[90/0/90]_s$ laminated shell with an outer stiffening ring ($c_r = 3$ cm) of three different thicknesses are listed in Table 3. The comparisons of modal frequencies of the $[90/0/90]_s$ laminated shell with an outer stiffening ring ($b = 3$ cm) of three different widths are listed in Table 4. The shape of cross-section for both the laminated shell and the ring does not change for the mode (1, 0). The cross-section of both the laminated shell and the ring for the mode (1, 1) is in the state of rigid body motion. In this situation, the ring adds a mass to the combined structure. As a result, either the thicker ring or the wider ring imply both smaller ω_{10} and ω_{11} of the combined structure. Although the ring is located at the nodal line of the laminated shell for the modes (2, 1) and (2, 2), the ring induces a countered moment at the connection of ring and laminated shell. As a result, the laminated shell stiffened with either the wider ring or the thicker ring is more difficult to be deformed in the transverse direction for $i = 2$. Therefore, either the thicker ring or the wider ring implies both larger ω_{21} and ω_{22}. Either the thicker ring or the wider ring gives a more constraint on the deformation of cross-section of the laminated shell for the mode (1, 2). Therefore, either the thicker ring or the wider ring implies larger ω_{12}.

The comparisons of two different lamination schemes $[0/90/0]_s$ and $[90/0/90]_s$ on the modal frequencies of the laminated shell with an outer stiffening ring ($b = c_r = 3$ cm) are displayed in Table 5. The $[0/90/0]_s$ laminated shell has larger bending rigidity, however, smaller transverse shear stiffness than the $[90/0/90]_s$ laminated shell does. Therefore, the $[0/90/0]_s$ laminated shell with an outer stiffening ring has both larger ω_{11} and ω_{21}, however, both smaller ω_{12} and ω_{22} than those of the $[90/0/90]_s$ laminated shell with an outer stiffening ring.

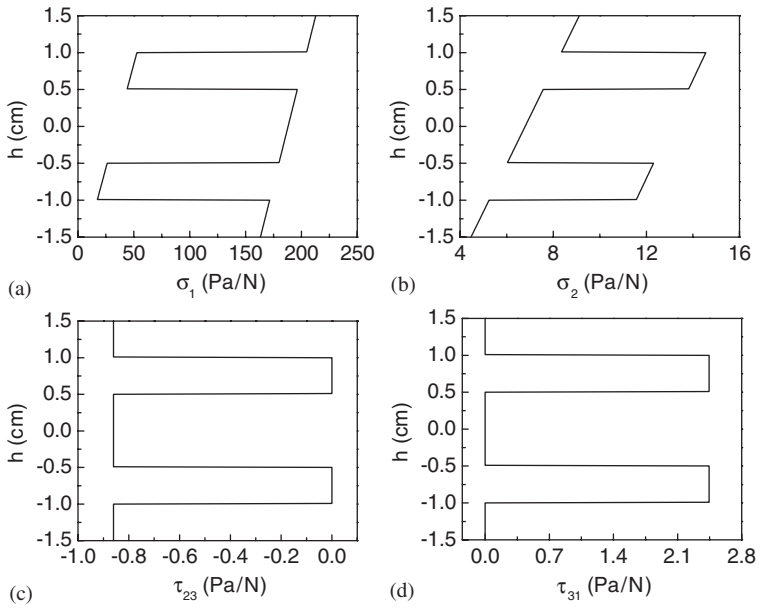

Fig. 9. The stress distributions in thickness along the line of an acting force on the $[90/0/90]_s$ laminated shell ($a = 30$ cm) with an outer stiffening ring: (a) σ_1, (b) σ_2, (c) τ_{23}, and (d) τ_{31}.

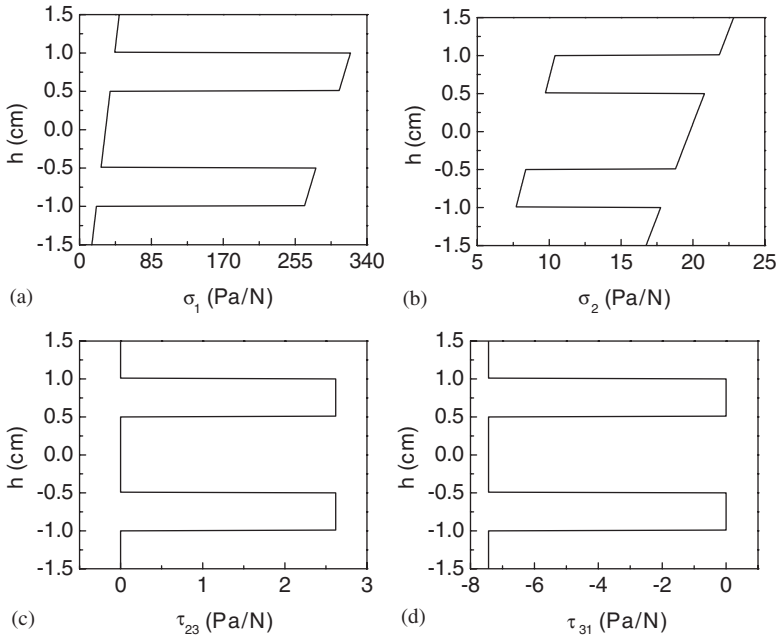

Fig. 10. The stress distributions in thickness along the line of an acting force on the $[0/90/0]_s$ laminated shell ($a = 30$ cm) with an outer stiffening ring: (a) σ_1, (b) σ_2, (c) τ_{23}, and (d) τ_{31}.

The stress distributions in the $[90/0/90]_s$ laminated shell with an outer stiffening ring are plotted in Figs. 9(a)–(d) for σ_1, σ_2, τ_{23} and τ_{31}, respectively. The stress distributions in the $[0/90/0]_s$ laminated shell with an outer stiffening ring are displayed in Figs. 10(a)–(d) for σ_1, σ_2, τ_{23} and τ_{31}, respectively. Results listed in Figs. 9(a)–10(d) demonstrate that the $[0/90/0]_s$ laminated shell bears greater maximum stresses than the $[90/0/90]_s$ laminated shell does. Based on the failure criteria of maximum stress, the first failure will occur at

Table 6
The thickness b (cm) effect of inner ring ($c_r = 3$ cm) on the comparison of the modal frequencies (rad/s) of the ring-stiffened $[90/0/90]_s$ laminated shell ($L_1 = L_2 = 2.5$ m, $a = 30$ cm, $h = 3$ cm)

b	ω_{10}	ω_{11}	ω_{21}	ω_{12}	ω_{22}
1	3746.9	723.4	1543.4	2151.3	2259.6
2	3735.6	721.0	1546.0	2173.0	2260.4
3	3724.6	718.8	1548.1	2205.0	2260.7

Table 7
The width c_r (cm) effect of inner ring ($b = 3$ cm) on the comparison of the modal frequencies (rad/s) of the ring-stiffened $[90/0/90]_s$ laminated shell ($L_1 = L_2 = 2.5$ m, $a = 30$ cm, $h = 3$ cm)

c_r	ω_{10}	ω_{11}	ω_{21}	ω_{12}	ω_{22}
3	3724.6	718.8	1548.1	2205.0	2260.7
6	3690.8	711.7	1556.9	2230.3	2268.9
9	3657.6	704.8	1567.9	2242.9	2279.4

Table 8
The layers effect on the comparison of the modal frequencies (rad/s) of the laminated shell ($L_1 = L_2 = 2.5$ m, $a = 30$ cm, $h = 3$ cm) with an inner stiffened ring ($b = 3$ cm, $c_r = 6$ cm)

Layer	ω_{10}	ω_{11}	ω_{21}	ω_{12}	ω_{22}
$[0/90/0]_s$	4737.2	790.4	1662.0	1559.7	1658.6
$[90/0/90]_s$	3690.8	711.7	1556.9	2230.2	2268.9

the sixth ply of the $[0/90/0]_s$ laminated shell and at the fifth ply of the $[90/0/90]_s$ laminated shell due to σ_2. Further, the sixth ply of the $[0/90/0]_s$ laminated shell is easier than the fifth ply of the $[90/0/90]_s$ laminated shell to be broken down.

7.3. Inner ring

The comparisons of modal frequencies of the $[90/0/90]_s$ laminated shell with an inner stiffening ring ($c_r = 3$ cm) of three different thicknesses are listed in Table 6. The comparisons of modal frequencies of the $[90/0/90]_s$ laminated shell with an inner stiffening ring ($b = 3$ cm) of three different widths are listed in Table 7. Results of Tables 6 and 7 indicate that either the thicker ring or the wider ring will imply both smaller ω_{10} and ω_{11}, however, larger ω_{12}, ω_{21} and ω_{22} of the combined structure.

The comparison of two different lamination schemes $[0/90/0]_s$ and $[90/0/90]_s$ on the modal frequencies of laminated shell with an inner stiffening ring ($b = c_r = 3$ cm) is displayed in Table 8. The $[0/90/0]_s$ laminated shell has larger bending rigidity, however, smaller transverse shear stiffness. Therefore, the $[0/90/0]_s$ laminated shell with an inner stiffening ring has larger ω_{10}, ω_{11} and ω_{21}, however, smaller ω_{12} and ω_{22} than those of the $[90/0/90]_s$ laminated shell with an inner stiffening ring.

The comparison of two kinds of stiffening rings on the modal frequencies are listed in Tables 9 and 10 for the ring-stiffened $[90/0/90]_s$ laminated shell and the ring-stiffened $[0/90/0]_s$ laminated shell, respectively. A stiffening ring adds a mass to the to the laminated shell for the modes (1, 0) and (1, 1). Further, an inner ring adds a smaller mass to the laminated shell for the modes (1, 0) and (1, 1). Therefore, both ω_{10} and ω_{11} of the laminated shell stiffened with an inner ring are greater than those of the same shell with an outer ring. Results of both tables also indicate that both outer ring and inner ring give a better effect on stiffening the laminated

Table 9
The rings ($b = 3\,\text{cm}$, $c_r = 6\,\text{cm}$) effect on the comparison of modal frequencies (rad/s) of the ring-stiffened $[90/0/90]_s$ laminated shell ($L_1 = L_2 = 2.5\,\text{m}$, $a = 30\,\text{cm}$, $h = 3\,\text{cm}$)

Ring	ω_{10}	ω_{11}	ω_{21}	ω_{12}	ω_{22}
No	3754.8	725.4	1542.0	2143.2	2257.9
Outer	3676.5	708.6	1565.3	2194.2	2283.1
Inner	3690.8	711.7	1556.9	2230.2	2268.9

Table 10
The rings ($b = 3\,\text{cm}$, $c_r = 6\,\text{cm}$) effect on the comparison of the modal frequencies (rad/s) of the ring-stiffened $[0/90/0]_s$ laminated shell ($L_1 = L_2 = 2.5\,\text{m}$, $a = 30\,\text{cm}$, $h = 3\,\text{cm}$)

Ring	ω_{10}	ω_{11}	ω_{21}	ω_{12}	ω_{22}
No	4906.7	805.1	1655.0	1427.8	1653.7
Outer	4695.2	787.1	1667.7	1530.2	1673.0
Inner	4737.2	790.4	1662.0	1559.7	1658.6

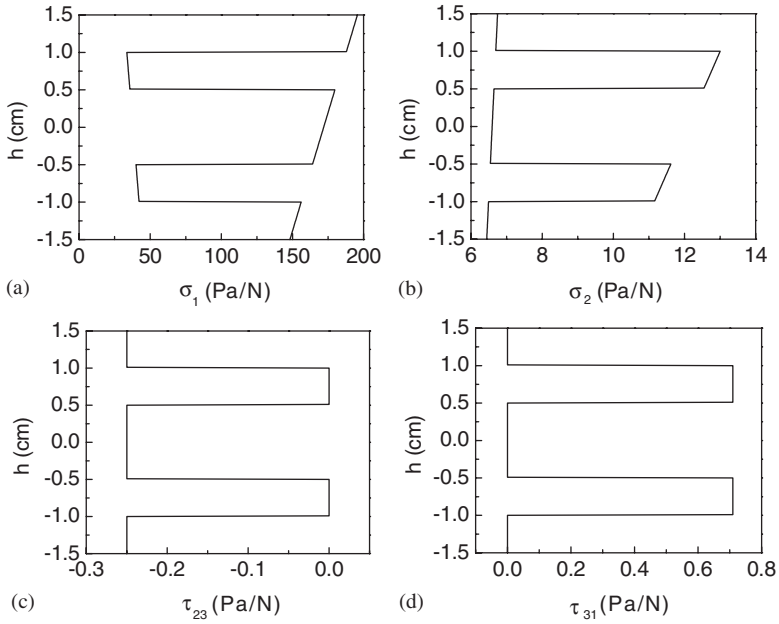

Fig. 11. The stress distributions in thickness along the line of an acting force on the $[90/0/90]_s$ laminated shell ($a = 30\,\text{cm}$) with an inner stiffening ring: (a) σ_1, (b) σ_2, (c) τ_{23}, and (d) τ_{31}.

shell for the modes (2, 1), (1, 2) and (2, 2). The outer ring gives a more constraint on countered moment than the inner ring does. Therefore, the outer ring gives a better effect on stiffening the laminated shell for the modes (2, 1) and (2, 2). However, the inner ring gives a more constraint on the transverse deformation of the laminated shell for the modes (1, 0), (1, 1) and (1, 2). Consequently, the inner ring gives a better effect than the outer ring on stiffening the laminated shell for the modes (1, 0), (1, 1) and (1, 2).

The stress distributions in an inner ring-stiffened $[90/0/90]_s$ laminated shell are plotted in Figs. 11(a)–(d) for σ_1, σ_2, τ_{23} and τ_{31}, respectively. The stress distributions in an inner ring-stiffened $[0/90/0]_s$ laminated shell are displayed in Figs. 12(a)–(d) for σ_1, σ_2, τ_{23} and τ_{31}, respectively. Results listed in Figs. 11(a)–12(d) demonstrate

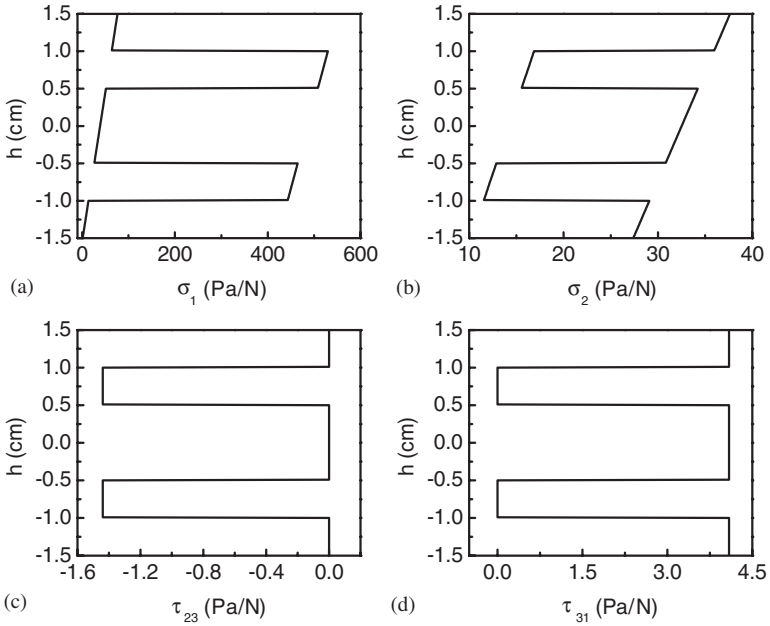

Fig. 12. The stress distributions in thickness along the line of an acting force on the $[0/90/0]_s$ laminated shell ($a = 30$ cm) with an inner stiffening ring: (a) σ_1, (b) σ_2, (c) τ_{23}, and (d) τ_{31}.

that the $[0/90/0]_s$ laminated shell bears greater maximum stresses than the $[90/0/90]_s$ laminated shell does. Based on the failure criteria of maximum stress, the first failure will occur at the sixth ply of the $[0/90/0]_s$ laminated shell and at the fifth ply of the $[90/0/90]_s$ laminated shell due to σ_2. Further, the sixth ply of the $[0/90/0]_s$ laminated shell is easier than the fifth ply of $[90/0/90]_s$ laminated shell to be broken down.

8. Conclusions

Based on the present modal analysis for the vibration of ring-stiffened cross-ply laminated cylindrical shells, the following conclusions can be made: (1) adding a ring to the shell will soften the combined structure for the modes (1, 0) and (1, 1); (2) adding a ring to the shell will stiffen the combined structure for the modes (2, 1), (1, 2) and (2, 2); (3) an outer ring gives a better effect than the inner ring on stiffening the combined structure for the modes (2, 1) and (2, 2); (4) an inner ring gives a better effect than the outer ring on stiffening the combined structure for the mode (1, 2); (5) the first failure is easier to occur in the ring-stiffened $[0/90/0]_s$ shell; and (6) the first failure is easier to occur in the $[0/90/0]_s$ shell with an inner stiffened ring.

Acknowledgment

This work was sponsored by the National Science Council, Republic of China, under Contract no. 92-2212-E-006-079. The financial support is gratefully acknowledged.

Appendix A. List of operators N_1–N_{17}

$$N_1 = aA_{11}^{(i)}\frac{\mathrm{d}^2}{\mathrm{d}x^2} - \frac{j^2}{a}A_{66}^{(i)} + \rho ah\omega^2, \tag{A.1}$$

$$N_2 = aA_{66}^{(i)}\frac{\mathrm{d}^2}{\mathrm{d}x^2} - \frac{1}{a}\left(j^2A_{22}^{(i)} + \kappa A_{44}^{(i)}\right) + \rho ah\omega^2, \tag{A.2}$$

$$N_3 = a\kappa A_{55}^{(i)}\frac{\mathrm{d}^2}{\mathrm{d}x^2} - \frac{1}{a}\left(j^2\kappa A_{44}^{(i)} + A_{22}^{(i)}\right) + \rho a h\omega^2, \tag{A.3}$$

$$N_4 = -aD_{11}^{(i)}\frac{\mathrm{d}^2}{\mathrm{d}x^2} + \frac{j^2}{a}D_{66}^{(i)} + a\kappa A_{55}^{(i)} - \rho a I\omega^2, \tag{A.4}$$

$$N_5 = -aD_{66}^{(i)}\frac{\mathrm{d}^2}{\mathrm{d}x^2} + \frac{j^2}{a}D_{22}^{(i)} + a\kappa A_{44}^{(i)} - \rho a I\omega^2, \tag{A.5}$$

$$N_6 = \frac{j}{a\kappa A_{55}^{(i)}}\left[\frac{1}{a}\left(A_{22}^{(i)} + \kappa A_{44}^{(i)}\right) + N_2\right], \quad N_7 = \frac{1}{a\kappa A_{55}^{(i)}}\left(j\kappa A_{44}^{(i)}c_2 + N_3\right), \tag{A.6,7}$$

$$N_8 = \left[c_1 N_5 - jc_3\left(D_{12}^{(i)} + D_{66}^{(i)}\right)\right]\frac{\mathrm{d}}{\mathrm{d}x}, \tag{A.8}$$

$$N_9 = j\left(D_{12}^{(i)} + D_{66}^{(i)}\right)N_6 - \kappa A_{44}^{(i)} - \frac{1}{\kappa A_{44}^{(i)}}N_2 N_5, \tag{A.9}$$

$$N_{10} = c_2 N_5 - j\kappa A_{44}^{(i)} - j\left(D_{12}^{(i)} + D_{66}^{(i)}\right)N_7, \tag{A.10}$$

$$N_{11} = j\left(D_{12}^{(i)} + D_{66}^{(i)}\right)c_1\frac{\mathrm{d}^3}{\mathrm{d}x^3} + c_3 N_4\frac{\mathrm{d}}{\mathrm{d}x}, \tag{A.11}$$

$$N_{12} = -N_4 N_6 - \frac{j\left(D_{12}^{(i)} + D_{66}^{(i)}\right)}{\kappa A_{44}^{(i)}}N_2\frac{\mathrm{d}^2}{\mathrm{d}x^2}, \tag{A.12}$$

$$N_{13} = \left[j\left(D_{12}^{(i)} + D_{66}^{(i)}\right)c_2 - a\kappa A_{55}^{(i)}\right]\frac{\mathrm{d}^2}{\mathrm{d}x^2} + N_4 N_7, \tag{A.13}$$

$$N_{14} = N_8\frac{\mathrm{d}}{\mathrm{d}x} - \frac{1}{A_{12}^{(i)}}N_{10}N_1, \quad N_{15} = N_9 - c_4 N_{10}, \tag{A.14,15}$$

$$N_{16} = N_{11}\frac{\mathrm{d}}{\mathrm{d}x} - \frac{1}{A_{12}^{(i)}}N_{13}N_1, \quad N_{17} = N_{12} - c_4 N_{13}, \tag{A.16,17}$$

in which

$$c_1 = j\frac{A_{12}^{(i)} + A_{66}^{(i)}}{\kappa A_{44}^{(i)}}, \quad c_2 = j\frac{A_{22}^{(i)} + \kappa A_{44}^{(i)}}{a\kappa A_{44}^{(i)}}, \quad c_3 = \frac{j\kappa A_{44}^{(i)}c_1 - A_{12}^{(i)}}{a\kappa A_{55}^{(i)}}, \quad c_4 = j\frac{A_{12}^{(i)} + A_{66}^{(i)}}{A_{12}^{(i)}}.$$

Appendix B. Arrays of the matrix $[K]_j$

$$k_{11} = \frac{A}{aR}\left(\rho_r R^2\omega^2 - j^2\kappa_r G_r\right), \quad k_{14} = k_{41} = -r_0 k_{11},$$

$$k_{22} = \frac{A}{aR}\left(\rho_r R^2\omega^2 - j^2 E_r - \kappa_r G_r\right), \quad k_{23} = k_{32} = -\frac{jA}{aR}(E_r + \kappa_r G_r),$$

$$k_{25} = k_{52} = \frac{\kappa_r G_r A}{a} + r_0 k_{22}, \quad k_{33} = k_{11} - \frac{E_r A}{aR}, \quad k_{35} = k_{53} = j\frac{\kappa_r G_r A}{a} + r_0 k_{32},$$

$$k_{44} = -r_0 k_{14} + \frac{1}{aR}\left(\rho_r J R^2 \omega^2 - j^2 D_r - E_r I_n\right),$$

$$k_{55} = r_0 k_{25} + \frac{A}{aR}\left[(r_0 - R)\kappa_r G_r R + \rho_r \frac{I_x}{A} R^2 \omega^2 - j^2 \frac{E_r I_x}{A}\right],$$

and others being zeros.

References

[1] T. Wah, W.C.L. Hu, Vibration analysis of stiffened cylinders including inter-ring motion, *Journal of the Acoustical Society of America* 43 (1968) 1005–1016.

[2] A.M. Al-Najafi, G.B. Warburton, Free vibration of ring-stiffened cylindrical shells, *Journal of Sound and Vibration* 13 (1970) 9–25.

[3] I.D. Wilken, W. Soedel, The receptance method applied to ring-stiffened cylindrical shells: analysis of modal characteristics, *Journal of Sound and Vibration* 44 (1978) 563–576.

[4] D.E. Beskos, J.B. Oates, Dynamic analysis of ring-stiffened circular cylindrical shells, *Journal of Sound and Vibration* 75 (1981) 1–15.

[5] G. Sinha, M. Mukhopadhyay, Transient dynamic response of arbitrary stiffened shells by the finite element method, *Journal of Vibration and Acoustics* 117 (1995) 11–16.

[6] B. Yang, J. Zhou, Analysis of ring-stiffened cylindrical shells, *Journal of Applied Mechanics* 62 (1995) 1005–1014.

[7] Y.W. Kim, Y.S. Lee, Transient analysis of ring-stiffened composite cylindrical shells with both edges clamped, *Journal of Sound and Vibration* 252 (2002) 1–17.

[8] Y. Xiang, Y.F. Ma, S. Kitipornchai, C.W. Lim, C.W.H. Lau, Exact solutions for vibration of cylindrical shells with intermediate ring supports, *International Journal of Mechanical Sciences* 44 (2002) 1907–1924.

[9] R.-T. Wang, Z.-X. Lin, Vibration analysis of ring-stiffened cylindrical shells, *Journal of the Chinese Society of Mechanical Engineers* 27 (2003) 583–594.

[10] H. Kraus, *Thin Elastic Shells*, Wiley, New York, 1967.

[11] J.R. Vinson, R.L. Sierakowski, *The Behavior of Structures Composed of Composite Materials*, Martinus Nijhoff Publishers, Dordrecht, 1986.

[12] S.P. Timoshenko, J.N. Goodier, *Theory of Elasticity*, McGraw-Hill, New York, 1970.

[13] R.-T. Wang, Vibration of a T-type curved frame due to a moving force, *Journal of Sound and Vibration* 215 (1998) 143–165.

[14] R.-T. Wang, J.-S. Lin, Vibration of multi-span Timoshenko frames due to moving loads, *Journal of Sound and Vibration* 212 (1998) 417–434.

[15] R.-T. Wang, Vibration of multi-span Timoshenko beams to moving force, *Journal of Sound and Vibration* 207 (1997) 731–742.

[16] W.S. David, Progressive failure analysis methodology for laminated composite structures, NASA TP-209107, 1999.